UiT
THE ARCTIC
UNIVERSITY
OF NORWAY

Faculty of Science and Technology
Department of Physics and Technology

Interplanetary dust fluxes observed with Parker Solar Probe

Emil Gorseth Henriksen

Master thesis in Space Physics, FYS-3931
June 2020

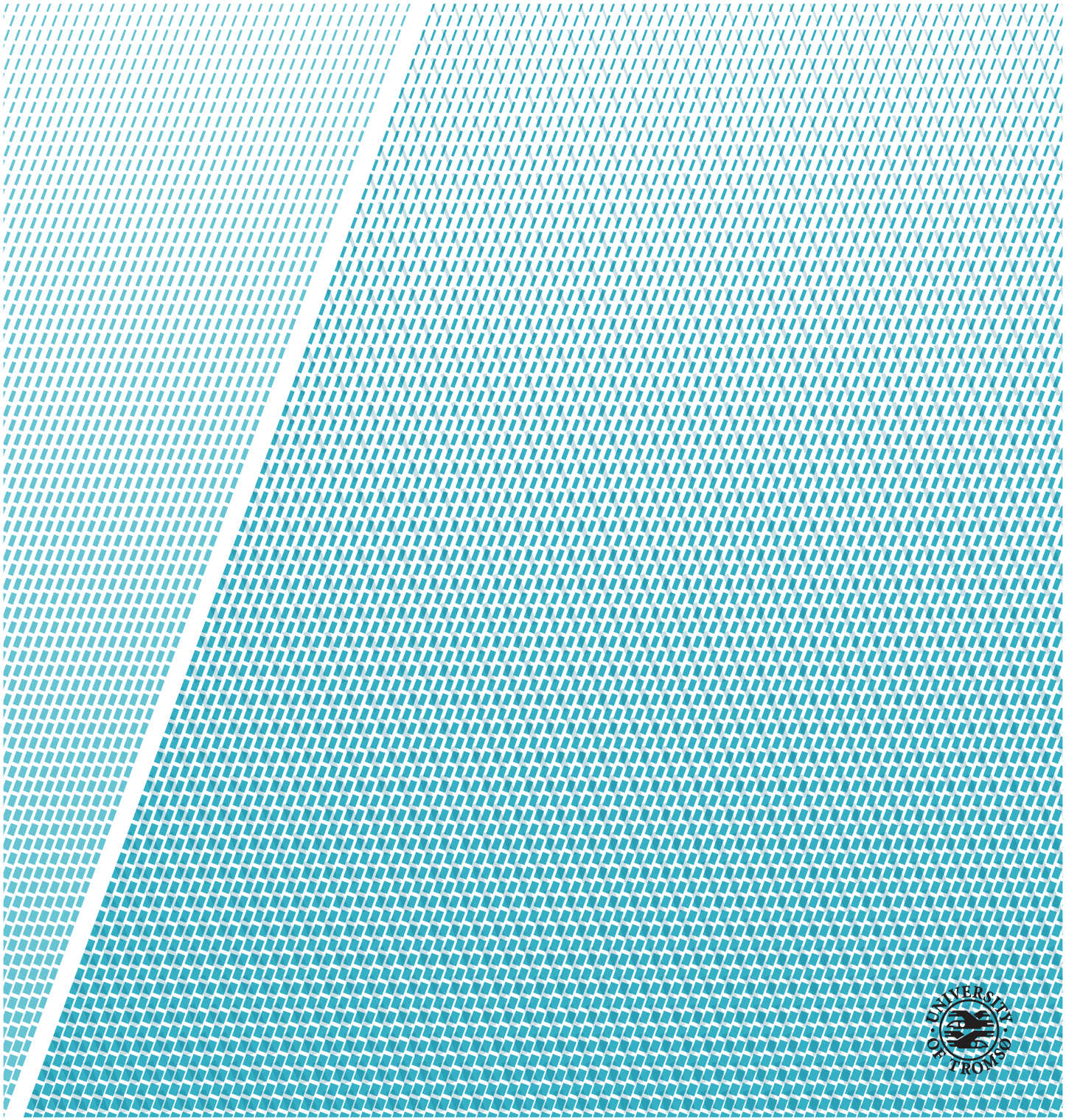

“Trust those who seek the truth, but doubt those who say they have found it.”
–André Gide

Abstract

The mission Parker Solar Probe (PSP) provides a new opportunity to make in-situ measurements of dust impacts closer to the Sun than ever before, eventually going as close as ~ 10 solar radii or ~ 0.05 AU. PSP can measure dust impacts from monopole measurements of the spacecraft's electric potential to one of its antennas using its FIELDS instrument. In this work impact rates data is compared to model calculations of dust flux at the spacecraft. The measurements are best described by dust particles forming inside of the PSP's orbit. The particles then move in hyperbolic orbits away from the Sun because they are repelled by the radiation pressure force. The dust particles can be pushed outward when the ratio of radiation pressure to gravity force exceeds 0.5. This ratio is often denoted as the beta value and the particles in unbound orbits as beta meteoroids.

In this thesis the dust impact rates measured by PSP during its second orbit are compared to calculated dust fluxes. The flux is influenced by the distance from the Sun, where the particles form, and their radiation pressure to gravity ratio ("beta value"). The finding of the range of these parameters result in well described impact rates. The radiation pressure to gravity ratio is found to be generally higher than previous studies. This suggests that PSP measures highly absorbing particles which could be dust particles freshly released from comets. An alternative suggestion is that the particles are not initially on circular orbits, but rather on highly elliptical orbits which will lead to a higher observed radiation pressure to gravity ratio. Three selected signals from monopole measurements are analyzed to derive dust particle parameters such as radiation pressure to gravity ratio and production distance. The signals are in agreement with beta meteoroids which are produced within 13 solar radii and with a radiation pressure to gravity ratio of above 1. It is shown that for the assumed dust impact signals an increase in production distance has to be met with an increase in the radiation pressure to gravity ratio. Similarly, if the particle is to be produced closer to the Sun it must have a smaller radiation pressure to gravity ratio.

Acknowledgements

I would like to thank my supervisor Professor Ingrid Mann and Dr Tarjei Antonsen for their invaluable help during my thesis work. This would not have been possible without them. Secondly, I thank Dr Audun Theodorsen and Saliha Eren for helpful discussions during my work, as well as Associate Professor Carol Norberg for proofreading and helpful comments.

Furthermore, I thank my fellow students for having someone to bother when I am feeling unproductive. It has certainly boosted my motivation having them beside me.

I also want to thank my family, and my dear Oda for their continued support.

Lastly, I thank NASA for providing free and public data access to FIELDS data from Parker Solar Probe. The FIELDS experiment on the Parker Solar Probe spacecraft was designed and developed under NASA contract NNN06AA01C.

Contents

List of Figures

1 Introduction

Scientists have known for a long time that the inner solar system contains dust (Zook and Berg, 1975). The dust can be seen with the naked eye by observing the zodiacal light on a late night or early morning. It can also be seen by observing the F-corona during a solar eclipse. The dust in the solar system has been analyzed through observational measurements as well as antenna measurements of different spacecraft orbiting the Sun, but never before have scientists been able to investigate the inner solar system through in-situ measurements in the same way that Parker Solar Probe (PSP) allows (McComas et al., 2007). The probe will go closer to the Sun than any man-made object has ever gone before. This will hopefully drastically improve our understanding of the inner solar system. Previous works on estimating dust population within the inner solar system are based on brightness observations and on in-situ measurements outside 0.3 AU[1] (Mann et al., 2004). With PSP these estimates can hopefully be updated to more reliable results.

PSP is expected to enter a harsh environment where the radiation from the Sun is extremely intense, as well as being on the boundary of where we expect the dust density of our inner solar system to be at its maximum. It is expected that the dust density increases up to a dust-free zone inwards from around 5 R_{Sun} due to sublimation (Mann et al., 2004). Since PSP is going to a distance of ~10

1. 1 AU is the average distance between the Sun and the Earth and is equal to $1.496 \cdot 10^{11}$ m or approximately 215 solar radii. The average radius of the Sun is $R_{sun} = 6.96 \cdot 10^{8}$ m or approximately 0.005 AU.

R_{Sun}, it is expected to undergo a number of dust impacts on to its antennas and body. It is these dust impacts scientists intend to measure and use to describe the environment better than previously possible.

This thesis focuses on analyzing the fluxes of beta meteoroids observed with PSP. An overview of the PSP mission is given in chapter 2, whereas chapter 3 describes beta meteoroids and their velocity components are derived. The process of detecting dust with antenna measurements on spacecraft is described in chapter 4. Chapter 5 introduces a dust flux model which will be used to calculate dust fluxes before comparing them to PSP's observations. In chapter 6 the results of calculated impact rates are presented and compared to measurements from PSP's second orbit. An error analysis is done to show how different models can explain the observations. Lastly, three selected monopole signals from PSP's first orbit are analyzed to estimate beta meteoroid parameters. Chapter 7 concludes the work and discusses what could be done in the future. Appendix A contains abstracts from previous work in addition to Python code for the calculations in this work. This thesis is an extension of the authors previous work, a project paper (Henriksen, 2019a) and special curriculum (Henriksen, 2019b) carried out during the autumn of 2019.

The position data of PSP was downloaded from the Parker Solar Probe Science Gateway, using the position calculator tool. FIELDS dust impact signal data was downloaded from http://research.ssl.berkeley.edu/data/psp/data/sci/fields/l2/. Dust impact rates data for the second orbit was kindly provided by Dr Jamey Szalay, Department of Astrophysical Sciences, Princeton University. The monopole data from the first orbit, containing assumed dust impact signals, was kindly pointed out by Dr Jakub Vaverka, Department of Surface and Plasma Science, Charles University in Prague.

2

Mission overview

PSP is a spacecraft mission made by NASA to investigate the inner solar system conditions and the corona of the Sun. The main goal of the mission is to investigate the solar wind and how it is accelerated to its high speed in the corona of the Sun (Fox et al., 2016). PSP carries with it several instruments for studying the solar wind and the corona such as ISIS, SWEAP and WISPR. PSP also has the FIELDS instrument to record electromagnetic field variations, plasma density, electron temperature and density fluctuations (Bale et al., 2016). It is this instrument that can be used for dust detection. FIELDS and its properties are more closely examined in chapter 4.

The spacecraft was launched on the 12th of August 2018, and will use seven Venus flybys to close in on the Sun, eventually reaching a minimum perihelion distance of about 10 R_{Sun}. The probe's first perihelion was on the 6th of November 2018 at 03:27 UTC, reaching a minimum distance of 35.7 R_{Sun}. The second perihelion was on the 4th of April 2019 (NASA, 2019). The dust flux observed during the second orbit will be discussed in this thesis. The orbit can be approximated with an ellipse with the following parameters: eccentricity of 0.6994 and semi-major axis of 0.5520 AU. The inclination to the ecliptic plane is 3.361 degrees and does not vary by more than 0.1 degree for all orbits (Szalay et al., 2020). Figure 2.1 shows orbit 2 of PSP in comparison to Earth orbit.

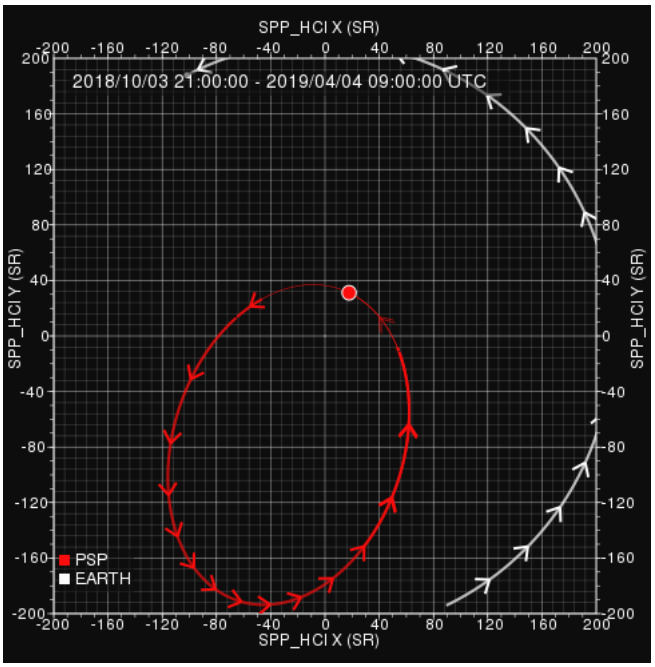

Figure 2.1: Orbit 2 of Parker Solar Probe shown in red, Earth orbit shown in white. This is a 2-D plot of the ecliptic plane in the HCI coordinate system, with the Sun in the center. The red dot shows PSPs position on the 4th of April 2019. Figure produced from the orbit plotting tool at https://sppgway.jhuapl.edu/.

2.1 Coordinate systems

In this work the coordinate systems used are the Heliocentric Inertial (HCI) and the Heliocentric Earth Ecliptic (HEE). The HCI coordinate system is suitable for plotting orbits, since they give an intuitive look on how the positions of objects relate to each other. In this coordinate system the z-axis is the solar rotational axis, and the x-axis is the solar ascending node on the ecliptic. The HEE coordinate system is convenient when working with the ecliptic since the z-axis points towards the ecliptic north-pole. Thus all motion in the x-y plane of the coordinate system is constrained to the ecliptic plane. The x-axis is the Sun-Earth line, which means the coordinate system rotates with time, which can make it less intuitive to imagine object orbits. An orbit in this coordinate system is not round, but rather a bell shaped curve (see figure 5.3 in section 5.5).

3

Beta meteoroids

This chapter introduces the concept of beta meteoroids. The dynamics of beta meteoroids and how they are produced in the vicinity of the Sun are presented. Their orbits and assumptions are discussed, as well as the velocity profiles for different beta meteoroids. Lastly their velocity components are derived.

3.1 Dust dynamics

Dust inside of Earth orbit is mostly produced within 1 AU, at small distances from the Sun. The dust particles can be released by comets and asteroids because of surface erosion or gas emission, or by collisional fragmentation between comets, asteroids and dust particles. The production is determined by the collision rate of larger meteoroids, and it depends on the number density and the relative velocities, which both increase closer to the Sun. The Poynting-Robertson effect also provides a source for dust particles in the inner solar system because it will slow down dust particles orbiting the Sun, bringing them to smaller and more circular orbits (Mann et al., 2004). The dust particles are large enough such that the main forces that act upon them are gravity and the solar photon momentum transfer which is the radiation pressure force. The radiation pressure force affects large particles mainly through the Poynting-Robertson effect. The momentum from the photons are transferred to the grains and in the frame of reference of the particle, the photons are coming in at an angle that is not perpendicular to the velocity vector of the grain. This creates a momentum transfer with a component antiparallel to the direction of the particles velocity, effectively slowing the particle down, and making its eccentricity and semi-major axis smaller. The effect of this is the particle slowly spiraling in towards the Sun, and trapping it in the dust cloud around the Sun and it is called the Poynting-Robertson effect.

Most of the dust particles are within 30° of latitude in the ecliptic, following the orbits of their parent object. Smaller charged dust particles however, are affected by magnetic field forces, and will be moved in the latitudinal direction. Very close to the Sun ($< 10\ R_{sun}$), particles below a size of 10 µm will be affected, and particles of size $0.5 - 2$ µm are strongly affected by magnetic field forces (Mann et al., 2004). These can be driven up to 90° in the latitude, meaning they can form a spherical dust cloud around the Sun.

The focus of this work is beta meteoroids, which can have the radiation pressure force working as their dominant force. Dust particles collide with each other and produce smaller fragments which are more strongly affected by the radiation pressure force and can escape the inner solar system on hyperbolic orbits. β is the ratio of radiation pressure force to the gravity force:

$$\beta = \frac{F_{rad}}{F_g} \tag{3.1}$$

The force can be approximated for sufficiently small perfectly absorbing objects as:

$$F_{rad} = P_{Sun}/c = L_{Sun} \cdot S/4\pi d^2 \tag{3.2}$$

where c is the speed of light, L_{Sun} is the luminosity of the Sun, S is the surface

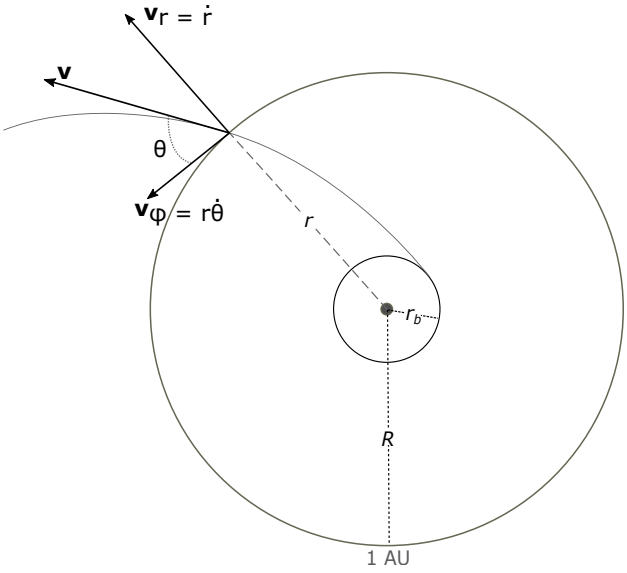

Figure 3.1: The trajectory of a beta meteoroid that is released from parent object in circular orbit with radius r_b and vectors showing the velocity components as it crosses an arbitrary distance, here at 1 AU. Figure adapted from Zook and Berg (1975).

of the absorbing object, and d is the distance from the Sun (Meyer-Vernet, 2007). The force has the same distance dependence as gravity, and so these two forces will provide the particle with constant acceleration.

The beta meteoroids are assumed to start out with the same orbital parameters and angular momentum as their parent particle upon production. When they are produced they quickly gain speed directed radially outward, and their azimuthal speed quickly decreases. The orbits of beta meteoroids are thus strongly determined by their size and initial conditions such as the distance of which they are produced and orbit of parent particle. Figure 3.1 shows the geometry of a beta meteoroid production process. With the Sun in the center, the inner circle shows the orbit of the parent object. The circle at 1 AU is an approximation to Earth orbit. The beta meteoroid is produced upon collisional fragmentation, and the introduction of the radiation pressure force forces the particle outwards on a hyperbolic orbit. The distance where the particle is produced is r_b, and r is an arbitrary distance where the velocity vectors can be calculated as $v_r = \dot{r}$ and $v_\phi = r\dot{\theta}$, where θ is the angle between the azimuthal velocity component and the total velocity component.

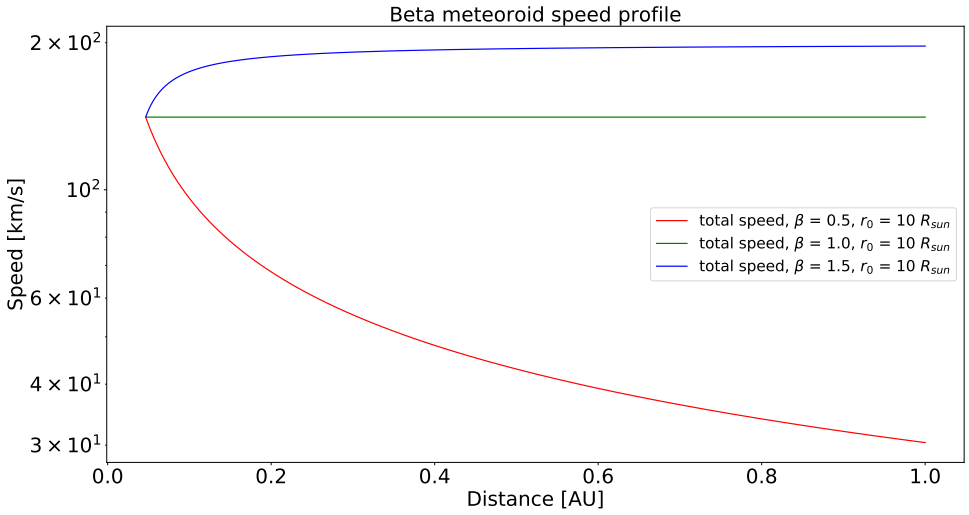

Figure 3.2: The speed as function of distance for particles released in circular orbit at 10 R_{Sun} and with radiation pressure to gravity ratios of 0.5, 1, and 1.5.

Figure 3.2 illustrates the velocities of particles that are influenced by the radiation pressure force. If $0.5 < \beta < 1$, the particle will slowly slow down while escaping the solar system on a hyperbolic orbit. At $\beta = 1$, the particle will have a constant speed exiting the solar system, and at $\beta > 1$ the particle gains speed as it exits the solar system.

Beta meteoroids are one of the sinks that empty the inner solar system of dust particles. Sublimation and sputtering are also mechanisms which destroy dust particles orbiting close to the Sun. Sputtering happens when the dust grain is so close to the Sun that the energetic solar wind particles hits the dust grain and ejects parts of atoms and molecules from that dust grain. The ejected particles are then contributing to the solar wind (Meyer-Vernet, 2007). Sublimation is the process where dust particles turn to gas without going through a liquid phase due to extreme temperatures. Mann et al. (2004) discusses different material composition of dust particles which can reach up to $2 - 3$ R_{sun} before sublimating. However, most particle compositions sublimate well before this. It is therefore assumed that most particles sublimate before or close to 5 R_{sun} and that there exists a dust-free zone within.

3.2 Beta meteoroids speed derivation

The expression for speed of a beta meteoroid was calculated by Zook and Berg (1975). Their approach to calculating the speed was followed, but it was discovered that the angular momentum was incorrectly defined in their derivation. Therefore, the derivation is included here to help eliminate confusion for future readers.
Starting with conservation of energy and angular momentum for a particle in motion about the Sun:

$$U = \frac{1}{2}\left(\dot{r}^2 + r^2\dot{\phi}^2\right) + V(r) \qquad h = r^2\dot{\phi} \tag{3.3}$$

where U is the total energy, V is the potential energy, h is the angular momentum per unit mass, r is the heliocentric distance, ϕ is the azimuthal angle, and the dot denotes the derivative with respect to time.
U and h are conserved, and V is given as:

$$V(r) = \frac{\mu}{r}(\beta - 1) \tag{3.4}$$

where β is the ratio between the radiation pressure and the gravity force and μ is the gravitational parameter equal to $G(M+m) \simeq GM = 1.38 \cdot 10^{20}$ $\mathrm{m^3\,s^{-2}}$.

Further, it is assumed that the beta meteoroid starts out with the same speed and angular momentum as its parent body, but its potential and total energy are changed due to β:

$$U_b = -\frac{1}{2}\frac{\mu}{r_b} \qquad V_b = -\frac{\mu}{r_b} \qquad h_b = v_b r_b = \sqrt{\mu r_b} \tag{3.5}$$

$$U_a = \frac{\mu}{r_b}\left(\beta - \frac{1}{2}\right) \qquad V_a = \frac{\mu}{r}(\beta - 1) \qquad h_a = h_b \tag{3.6}$$

The subscripts a and b correspond to before and after fragmentation.

The total speed is found by conservation of energy:

$$\begin{aligned} v_{R=1AU} &= \sqrt{2(U_a - V_a)} \\ &= \sqrt{2\mu\left[\frac{\beta - 0.5}{r_b} - \frac{\beta - 1}{R}\right]} \\ &= \sqrt{\frac{2\mu}{R}\left[\frac{\beta - 0.5}{(r_b/R)} - (\beta - 1)\right]} \end{aligned} \tag{3.7}$$

3.2.1 Calculating the azimuthal component

Applying conservation of angular momentum, the azimuthal speed of a beta meteoroid at any distance is derived. Initial speed is merely the circular orbital speed of the parent particle:

$$h_0 = r_0 v_{\phi 0} = r_0 \sqrt{\mu / r_0} = \sqrt{\mu r_0}$$

The angular momentum of the newly generated beta meteoroid is equal to the product of its heliocentric distance and its azimuthal velocity, and also equal to the angular momentum of the parent particle due to conservation of angular momentum:

$$h = r v_{\beta\phi} = h_0 = \sqrt{\mu r_0}$$

Solving for the azimuthal velocity of the new beta meteoroid yields:

$$v_{\beta\phi} = \frac{\sqrt{\mu r_0}}{r} \tag{3.8}$$

3.2.2 Calculating the radial component

Having the total speed of the beta-meteoroid and the azimuthal component, the radial component is found by

$$v_{\beta r} = \pm \sqrt{v_\beta^2 - v_{\beta\phi}^2} \tag{3.9}$$

To find the speed at any distance from the Sun, I insert r for R and set $r_b = r_0$:

$$v_\beta = \sqrt{2\mu \left[\frac{\beta - 0.5}{r_0} - \frac{\beta - 1}{r} \right]} \tag{3.10}$$

Inserting for equation 3.9 and using that for a beta meteoroid of $\beta > 0.5$ the radial speed is always positive:

$$\begin{aligned} v_{\beta r} &= \sqrt{2\mu \left[\frac{\beta - 0.5}{r_0} - \frac{\beta - 1}{r} \right] - \frac{\mu r_0}{r^2}} \\ &= \sqrt{2\mu \left[\frac{\beta - 0.5}{r_0} - \frac{\beta - 1}{r} - \frac{r_0}{2r^2} \right]} \end{aligned} \tag{3.11}$$

4

Dust detection

From Earth, dust can be detected by observing light scattered by the dust orbiting the Sun. Brightness measurements can be used to estimate the total amount of dust, size and some composition information. Spacecraft without dedicated dust detectors have also been used to detect dust, such as Voyager, WIND, Cassini and STEREO (Vaverka et al., 2017). Naturally, a spacecraft orbiting in space with dust surrounding it will eventually lead to collisions between the two. This has lead to scientists proposing a dust impact model, which explains the process of dust impacting the spacecraft, and leading to a measured signal which can be analyzed (Meyer-Vernet, 2001). The measurement is done by antenna instruments on board the spacecraft, which measure the electric potential between the spacecraft body and its antennas. The following sections will describe how the spacecraft is charged and how the dust impact process can be measured.

4.1 Spacecraft charging

The spacecraft is charged to a floating potential due to different currents. The main currents are the solar wind particle collection current and the photoelectric emission current (Whipple, 1981). The following information and impact model references Zaslavsky (2015). In addition to the solar wind particle collection current and the photelectric emission current, there is a secondary electron emission current. This is negligible unless the impacting electrons have an energy of several hundreds of electron volts. This can be found in magnetospheric regions of atmospheres, but is negligible in the solar wind. Thus an expression for the spacecraft charging can be written as:

$$\frac{dq}{dt} = I_{sw} + I_{ph} + I_{sec} + \dots \tag{4.1}$$

Where I_{sw} is the solar wind charging current, I_{ph} is the photoelectron charging current, I_{sec} is the current of secondary electrons, and the dots denote further possible components assumed to be negligible.

The solar wind particle collection current consists mainly of electrons charging the spacecraft, because the electrons impact the spacecraft with their thermal velocity, and the ions impact with the solar wind velocity. The relationship between the two is: $v_{th} >> v_{sw}$, meaning the thermal velocity of the electrons is much greater than the velocity of the solar wind. This charges the spacecraft negatively, thus it is working against the photoelectron current. The proton collection current is negligible since the spacecraft floats at a positive potential in the solar wind, and will repel positive charges. The electrons charging the spacecraft by the solar wind current are described by the orbit-limited assumption (Meyer-Vernet, 2007), and can be modeled as:

$$I_{sw} \simeq I_{e0}\left(1 + \frac{\phi}{T_e}\right)^{\alpha} \tag{4.2}$$

where $I_{e0} = -en_e v_e S$ is the current of electrons impacting the surface if the surface is not charged, ϕ is the electric potential of the spacecraft, T_e is the solar wind electron temperature and α is determined by the charging process' geometry. e is the elementary charge, n_e is the local electron density and S is the surface of the spacecraft that is being charged.

The spacecraft emits photoelectrons due to the photoelectric effect, which charges the spacecraft positively. The current of photoelectrons is given as:

$$I_{ph} \simeq I_{ph0}\left(1 + \frac{\phi}{T_{ph}}\right)^{\gamma} e^{-\phi/T_{ph}} \tag{4.3}$$

where $I_{ph0} = J_{ph0} S_{lit}$ is the current of photoelectrons generated when the

surface is illuminated, J_{ph0} is the photoemission current density, S_{lit} is the surface of the spacecraft lit by the Sun, γ is a parameter determined by the charging process' geometry and T_{ph} is the photoelectron temperature.

For the simplest case of $\alpha, \gamma = 0$ which Zaslavsky (2015) refers to as one-dimensional charging the equation describing the potential of the spacecraft can be solved by approximating the charge production to be in a steady state where all charging currents balance to zero, and solving for ϕ:

$$\begin{aligned}
\frac{dq}{dt} &= I_{e0} + I_{ph0} \cdot e^{-\phi/T_{ph}} = 0 \\
-\frac{I_{e0}}{I_{ph0}} &= e^{-\phi/T_{ph}} \\
\ln\left(-\frac{I_{e0}}{I_{ph0}}\right) &= -\frac{\phi}{T_{ph}} \\
\ln(-I_{e0}) - \ln\left(I_{ph0}\right) &= -\frac{\phi}{T_{ph}} \\
\frac{\phi}{T_{ph}} &= \ln\left(I_{ph0}\right) - \ln(-I_{e0}) \\
\phi &= T_{ph} \ln\left(\frac{J_{ph0} S_{lit}}{e n_e v_e S_{sc}}\right)
\end{aligned} \tag{4.4}$$

To further model the change in potential due to a short-time charging process (a dust impact) and assuming the potential change will be small in comparison to the potential of the spacecraft, an expression for the potential perturbation can be found as a convolution between a dust impact current and an exponential decay back to the floating potential:

$$\delta\phi = \frac{1}{C} \int_0^\infty e^{-t'/\tau} I_{dust}(t - t') dt' \tag{4.5}$$

where C is the capacitance of the spacecraft, τ is the relaxation time the spacecraft uses to reach its floating potential again after an impact, and I_{dust} is the dust impact current charging the spacecraft. The dust impact current is modeled as a Gaussian function where the width of the pulse is determined by the charging timescale, Δt, and the amplitude determined by the amount of charges produced, Q. The relaxation time is calculated as:

$$\tau_{sc} = \frac{C_{sc} T_{ph}}{e n_e v_e S_{sc}} \tag{4.6}$$

where C_{sc} is the capacitance of the spacecraft, T_{ph} is the photelectron temperature, e is the electron charge, n_e is the electron density of the surrounding solar wind, v_e is the electron thermal velocity and S_{sc} is the spacecraft surface.

As discussed in Henriksen (2019a), a sunlit conducting surface in space must charge to a positive potential, since the flux of photons by far outweighs the collected plasma particles from the solar wind. Similarly, a shadowed surface will charge to a negative potential since the electrons are moving much faster than the ions, and are collected on the surface of the object (Meyer-Vernet, 2007). This results in the spacecraft having a floating potential difference between its body and antenna, that varies with solar wind parameters and local plasma density variations.

4.2 Dust impacts

As the spacecraft orbits the Sun, it will collide with dust particles at a variable but often very high speed. Because of the high speed of the collision, the dust particle vaporizes upon impact with a part of the spacecraft body. This leaves a small crater, and the material that is vaporized ionizes into electrons and ions due to the extreme temperatures (Mann et al., 2019). A semi-empirical model of charge production has been determined from laboratory experiments, and it shows that $Q = a \cdot m^f v^g$ where a, f and g are determined by the materials of the spacecraft and dust composition, m is the mass of the dust grain in kg and v is the impact speed in km s^{-1} (Dietzel et al., 1973; McBride and McDonnell, 1999). For a spacecraft floating at a positive potential the electrons are attracted and the protons are repelled, leading to a sharp potential perturbation between the spacecraft body and its antennas. These perturbations are often many times bigger than local plasma variations, which make them stand out in the data. The electric potential of the spacecraft is charged back to the floating potential by the previously mentioned spacecraft charging currents. This process is seen in the electric potential data of the spacecraft. In this way dust impacts on to the spacecraft are observed.

As the spacecraft body has a many times bigger surface area than the antennas, the dust is most likely to impact the body itself. The potential difference between two antennas (dipole) will not be as affected by the dust impact as the potential difference between an antenna and the spacecraft body (monopole). This is why monopole measurements are preferred when doing dust impact detection. Figure 4.1 shows an ideal dust impact at 1 AU for a dust grain with charge production of 50 pC. It was calculated in my special curriculum (Henriksen, 2019b) using the model introduced in the previous section.

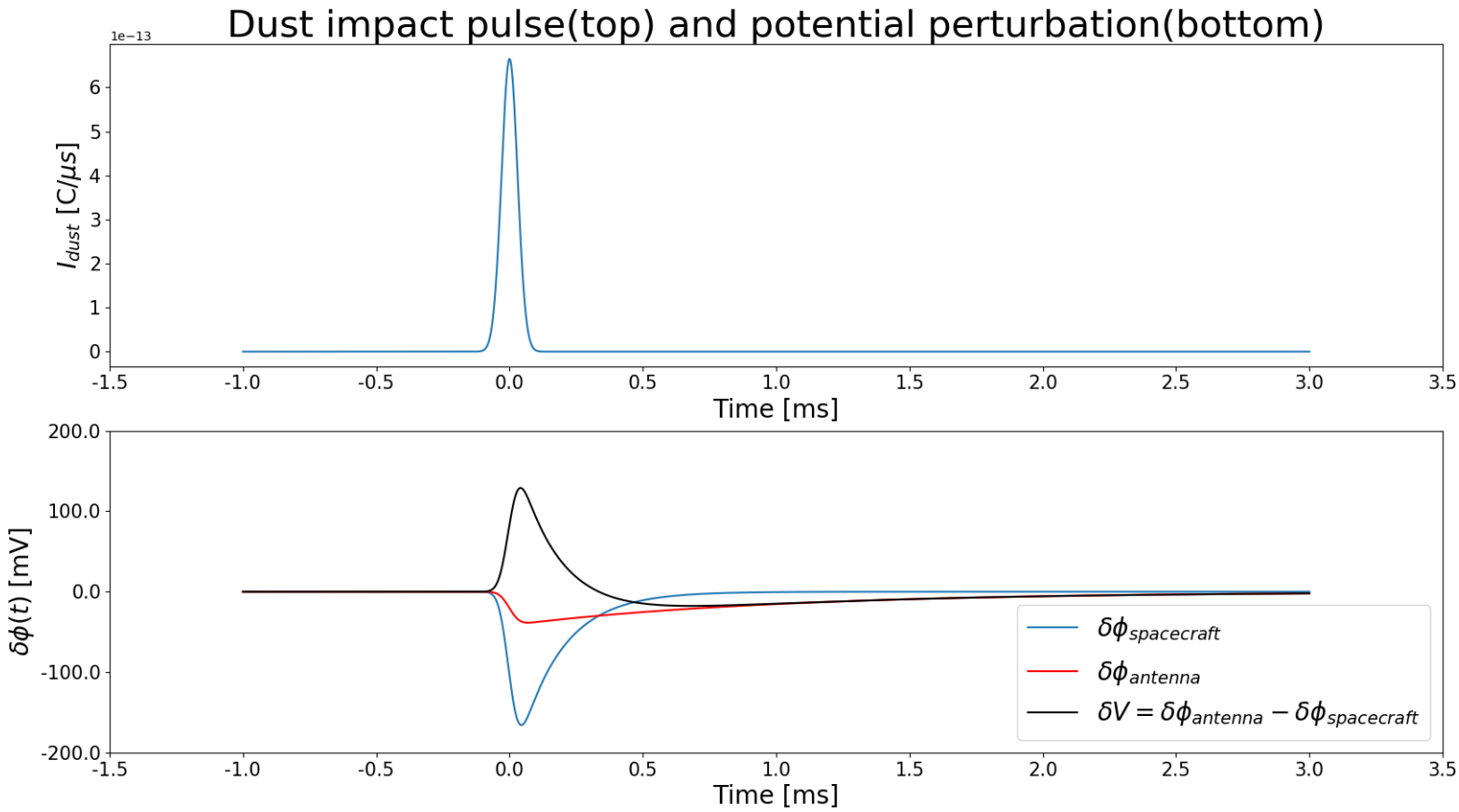

Figure 4.1: Top panel: Dust impact current I_{dust} for impact at 1 AU and 50 pC charge production. Bottom panel: Spacecraft floating potential perturbation due to dust impact pulse, and relaxation back to floating potential. Figure from Henriksen (2019b).

4.3 FIELDS instrument suite

The FIELDS instrument suite on PSP monitors magnetic and electric field variations. It consists of five antennas where four are mounted at the base of the heat shield and the fifth is at the back of the spacecraft. The four mounted at the base point outwards into the solar wind surrounding the spacecraft. The signals from the antennas are processed by the Digital Fields Board, a Time Domain Sampler (TDS) and the Radio Frequency Spectrometer. The Digital Fields Board can have a sample rate of up to 150 000 Hz, while the Time Domain Sampler can provide high resolution waveform data with a sample rate of up to 2 000 000 Hz. The signals with dust impacts will be automatically flagged to indicate such an event has occurred. The flags are triggered by several conditions. Half of them are triggered by peak or average amplitudes of the burst data, and the other half is triggered by external factors, e.g. magnetometer data or specific times (Malespina, 2020).

5

Dust flux model

In this chapter the dust flux model used to calculate beta meteoroid impact rates for PSP is introduced. The parameters that enter into calculating the dust fluxes are all described, the evolution of different beta meteoroids velocity is described, and the spacecraft's velocity components are derived.

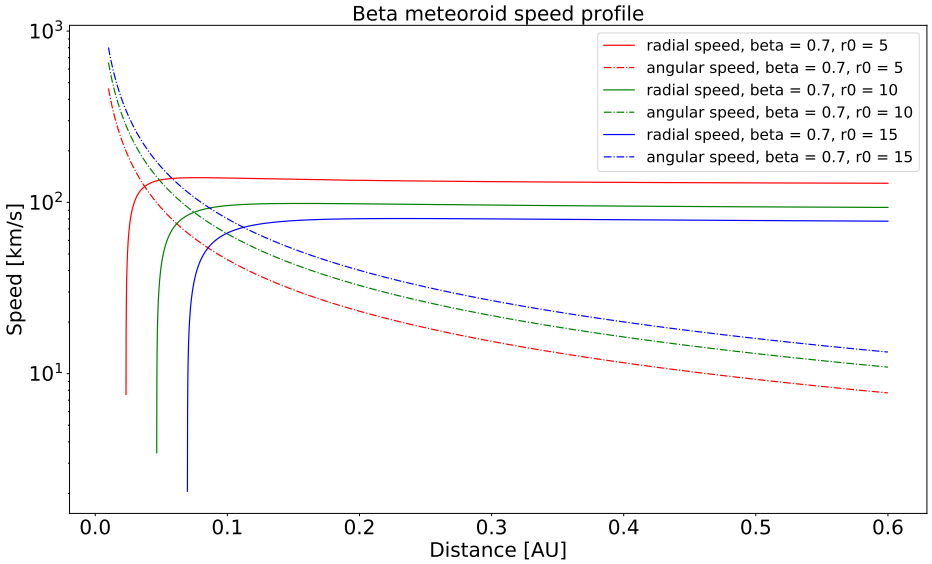

Figure 5.1: Speed profiles for beta meteoroids with $\beta = 0.7$ that are released at distances from the Sun $r_0 = [5, 10, 15]$ R_{sun}. The solid lines are the radial speed components, and the dash-dotted lines are the azimuthal speed components (called "angular" in figure). The red, green and blue colors refer to production distances of 5, 10 and 15 R_{sun} respectively.

5.1 Beta meteoroid impact rates

Since the suggested dust free zone starts at 5 R_{Sun}, the production of beta meteoroids is assumed to begin from 5 R_{Sun}, and continue outwards. It is not known where this region stops, but it would be natural to assume it continues further out than 20 R_{Sun}. However, as the density decreases so does the probability of a collision and the amount of particles produced, therefore, this work only focuses on dust produced between 5 and 20 R_{Sun}. Figure 5.1 shows that at distances larger than 0.1 AU the radial speed is the dominant component for the velocity of beta meteoroids that are released at distances $r_0 = 5$ and $r_0 = 10$ R_{sun}. For beta meteoroids released at $r_0 = 15$ R_{sun} the point where the radial component is the dominant one is further out, at around 0.13 AU.

The dust flux model used here assumes that the dust is produced at a given distance, meaning it is produced in a narrow band around the Sun. This is most probably not the case, but it is expected that comparing the model flux to the data will still point to a region in which most of the dust is produced.

The impact rates were calculated as:

$$R = n(r) \cdot v_{imp}(r) \cdot A \tag{5.1}$$

Where n is the number density of beta meteoroids, v_{imp} is the impact speed, r is the heliocentric distance and A is the projected area of PSP which is being hit by beta meteoroids. The following sections will explain how these parameters are estimated.

5.2 Density distribution

Brightness observations suggest that the larger dust particles that are in bound orbits have a number density distribution that varies with distance, r, from the Sun as $r^{-1.3}$ (Leinert et al., 1978). This relation does not fit well with observations by PSP when calculating the impact rates. It is therefore likely that the majority of dust impacts on PSP are not from dust in bound circular orbits. Szalay et al. (2020) provides an estimation of the expected radial scaling of beta meteoroids. They find that the number density of beta meteoroids with beta > 0.6 are approximated to be proportional to r^{-2} when outside 0.1 AU or $\sim 22\ R_{Sun}$ (see equation 12 and surrounding text of Szalay et al. (2020)). Since little is known of the density distribution inside 0.1 AU the same radial scaling is used inside 0.1 AU. This leads to the expression for the beta meteoroid number density:

$$n(r) = \frac{n_0}{(r/1\ \text{AU})^2} \tag{5.2}$$

Where n_0 is the measured dust density at 1 AU. All calculated models were scaled to fit the data at perihelion by changing the value for n_0.

5.3 Spacecraft orbit

For the analysis, data from the first and the second orbit of PSP was used. They are approximately elliptical orbits and they are different since the probes perihelion decreases for each orbit. The orbital parameters can still be approximated to be similar for the orbits, and are given as $e = 0.6994$ and $a = 0.5520$ AU. The inclination is also similar for both orbits, $i = 3.361°$(Szalay et al., 2020). In the following section the velocity components of PSP will be derived.

5.3.1 Spacecraft velocity components

Starting with the vis-viva equation for conservation of energy in the motion of orbiting bodies, the velocity v is given by:

$$v = \sqrt{\mu \left(\frac{2}{r} - \frac{1}{a} \right)} \tag{5.3}$$

where a is the semi-major axis of the orbit, μ is the same as previously used and r is heliocentric distance. Applying conservation of mass and angular momentum, the azimuthal velocity of an orbiting body becomes:

$$v_\phi = \frac{\sqrt{\mu a(1 - e^2)}}{r} \tag{5.4}$$

where e is the eccentricity of the orbit. This will be the azimuthal velocity component for the spacecraft.

The radial component is found similarly to the beta meteoroid case, by using equation 3.9:

$$\begin{aligned} v_r &= \mp \sqrt{\mu \left(\frac{2}{r} - \frac{1}{a} \right) - \frac{\mu a(1 - e^2)}{r^2}} \\ &= \mp \sqrt{\mu \left(\frac{2}{r} - \frac{1}{a} - \frac{a(1 - e^2)}{r^2} \right)} \end{aligned} \tag{5.5}$$

The negative expression is used on the inbound leg and the positive on the outbound leg.

The perpendicular velocity component is calculated from PSP position data in the HEE coordinate system. It is small compared to the other velocity components, as shown in figure 5.2. The vertical component is one order of magnitude less than the azimuthal component for almost the entire section of the orbit in question. However, the fact that it reaches a maximum at around day of the year (DOY) 95, which is close to perihelion, is interesting for the dust impact rates, suggesting PSP might experience more impacts during this period. The reason for the gap in the radial velocity component seen in the figure is that at perihelion the radial velocity naturally goes to zero, and the orbital parameters are a bit off since they are assumed to be equal for both orbits 1 and 2. This leads to a mathematical error in the calculation of the velocity for perihelion, which is why there is a gap.

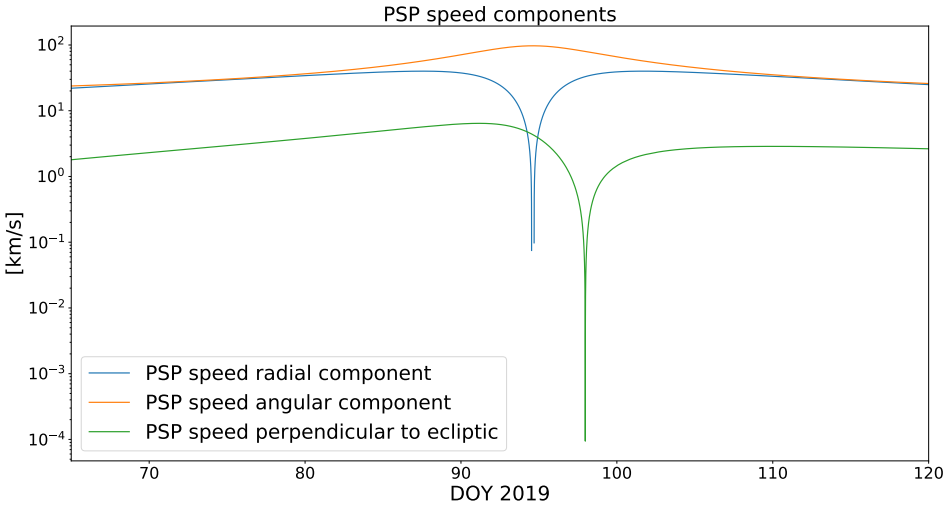

Figure 5.2: PSP velocity components during orbit 2. The perpendicular component is one order of magnitude smaller than the azimuthal ("angular" in the figure) component for the entire orbit.

5.4 Impact speed calculation

The most important factor for a dust impact, in addition to mass, is its impact speed. The impact speed is determined by the velocity of the spacecraft, the velocity of the dust particle, and the direction of these two velocities. The velocity of the spacecraft has been analytically derived, as well as the velocity of the beta meteoroids for different sizes and different parent orbits. The parent objects are assumed to be on circular orbits, and the fragments are assumed to start out with the same angular momentum and speed as the parent object.

The impact speed was calculated as:

$$\boldsymbol{v}_{imp} = \boldsymbol{v}_{\beta} - \boldsymbol{v}_{sc} \tag{5.6}$$

For the radial component this becomes:

$$v_{imp,r} = \sqrt{2\mu\left[\frac{\beta - 0.5}{r_0} - \frac{\beta - 1}{r} - \frac{r_0}{2r^2}\right]} \pm \sqrt{\mu\left(\frac{2}{r} - \frac{1}{a} - \frac{a(1-e^2)}{r^2}\right)} \tag{5.7}$$

Where the + signifies the spacecraft is inbound to perihelion, and − is outbound after perihelion.

Similarly, for the azimuthal component:

$$\begin{aligned} v_{imp,\phi} &= \frac{\sqrt{\mu r_0}}{r} - \frac{\sqrt{\mu a(1-e^2)}}{r} \\ &= \frac{\sqrt{\mu}}{r}\left(\sqrt{r_0} - \sqrt{a(1-e^2)}\right) \end{aligned} \tag{5.8}$$

Finally, the total impact speed is calculated as:

$$v_{imp} = \sqrt{v_{imp,r}^2 + v_{imp,\phi}^2 + v_z^2} \tag{5.9}$$

where v_z is PSPs vertical velocity component to the ecliptic plane. As previously mentioned it is small compared to the radial and azimuthal component, but it is included just in case it will make a difference on the impact speed. The reason it is only the spacecraft's velocity in this direction is because of the assumption that dust grains are constrained to motion within the ecliptic plane. Thus the impact speed in the vertical direction is simply the spacecraft's velocity in this direction.

5.5 Spacecraft surface

For calculating the impact rates onto PSP the area of impact has to be estimated. Here, the area is assumed to be constant during an orbit, and it is seen from equation 5.1 that it will linearly scale the impact rates. It was shown in figure 5.1 that at perihelion during orbit 2, the beta meteoroids will be moving dominantly in the radial direction. The orbits of beta meteoroids can be calculated from equations given in Wyatt (2009):

$$\begin{aligned} a_{new} &= a(1-\beta)\left[1 - 2\beta[1 + e\cos(f)][1-e^2]^{-1}\right]^{-1} \\ e_{new} &= [e^2 + 2\beta e\cos(f) + \beta^2]^{0.5}/(1-\beta) \end{aligned}$$

where a is the semi-major axis, e is the eccentricity of the orbit and f is the true anomaly at the point of production. These orbits are shown in figure 5.3.

Previous work (Calvinhac, 2019; Szalay et al., 2020; Henriksen, 2019a) shows that even though the probe will by flying in a similar direction to the beta meteoroids after perihelion, most impacts will be from particles coming radially outward from the Sun. Figure 5.3 shows orbits of beta meteoroids with $\beta = 0.6$ produced uniformly around the Sun at 10 R_{Sun} crossing PSP's orbit in the HEE coordinate system. Considering PSP's heat shield will be pointing towards the Sun at all times, it is reasonable to assume that most beta meteoroids will impact the heat shield of PSP. It is assumed that the area can not increase or

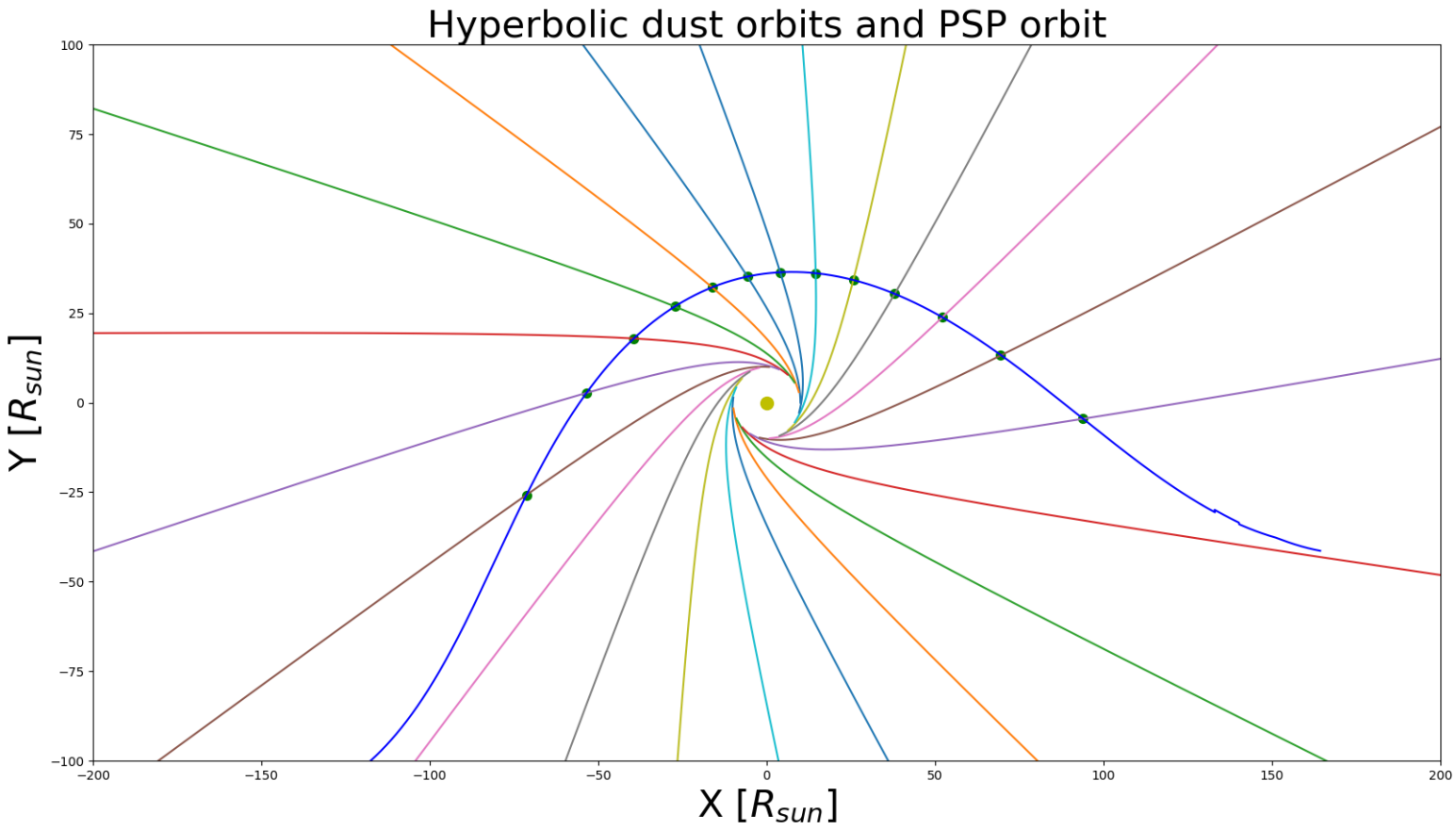

Figure 5.3: PSP's orbit in the HEE coordinate system. Orbits of beta meteoroids with $\beta = 0.6$ produced uniformly around the Sun at 10 R_{Sun} are shown in different colors. PSP's orbit is shown in dark blue, and the points along the orbit show dust impacts. Figure adapted from Henriksen (2019a).

decrease drastically during an orbit, such that the error would at its maximum be a factor of 2. This factor is acceptable since the impact rates are anyhow scaled (by n_0) to fit the data.

6

Results

This chapter introduces the results from using the models described previously to estimate the flux of beta meteoroids impacting PSP during its second orbit. An error analysis is done to visualize what models best can describe the data. Lastly, three selected monopole signals assumed to be dust impacts are analyzed to estimate parameters of the beta meteoroids producing these signals.

6.1 Impact speed

Figure 6.1 shows the calculated impact speeds for beta meteoroids of different radiation pressure to gravity ratios and different production distances. They were calculated from equations 5.7 − 5.9. The solid lines show impacts speeds calculated for beta meteoroids produced at 5 R_{sun}, the dotted lines show impact speeds for beta meteoroids produced at 10 R_{sun} and the dash-dotted lines show impact speeds for beta meteoroids produced at 15 R_{sun}. The colors blue, green and yellow correspond to $\beta = [0.5, 0.7, 1.2]$, respectively.

Models with $\beta = 0.5$ stand out with the lowest impact speeds. Their shape differs from the other models, being steeper both on the inbound and the outbound leg of PSP's second orbit. The other cases where $\beta = [0.7, 1.2]$ the impact speed is almost constant on the inbound leg, and it does not have a peak in perihelion as for $\beta = 0.5$. The impact speeds dip down to a lower value after perihelion and keep their linear trend.

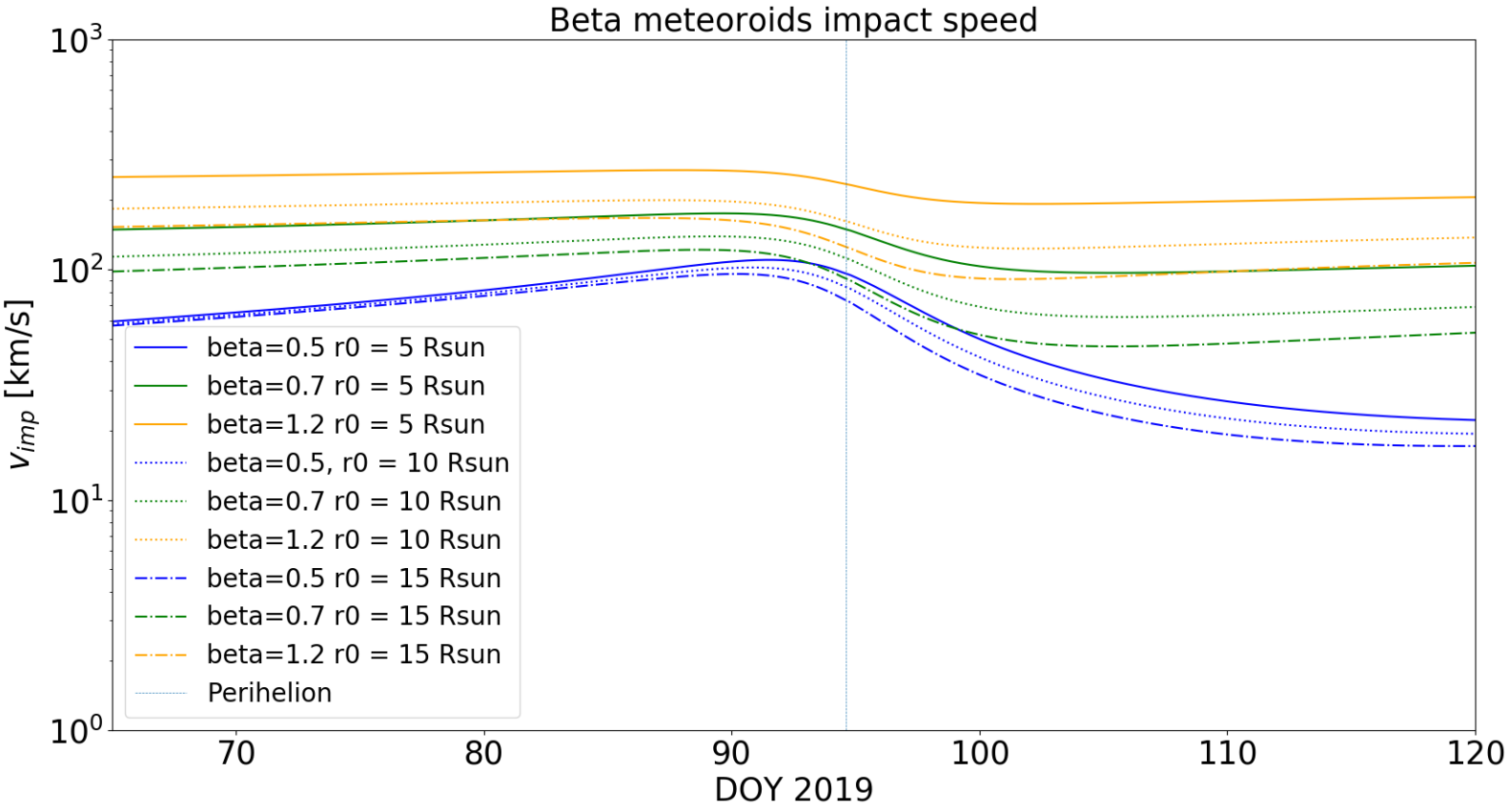

Figure 6.1: Impact speeds for different beta meteoroids. Blue lines have $\beta = 0.5$, green lines have $\beta = 0.7$ and the yellow lines have $\beta = 1.2$. The impact speeds are calculated for a beta meteoroid production distance from the Sun of 5, 10 and 15 R_{Sun}.

6.2 Impact rates

The impact rates were calculated for different β and r_0 using equation 5.1. They are presented in figure 6.2 together with the observed impact rates of PSP's second orbit. All flux curves were scaled by n_0 to fit the TDS impact rates at perihelion. One can see that the impact rates for $\beta = 0.5$ stands out again. They are least similar to the data because they have a too steep slope. Models where the radiation pressure to gravity ratio is higher than 0.5 are similar to each other on the inbound leg and at perihelion, but separate on the outbound leg. It is also seen that most models fail to fit the linear trend on the inbound leg. All models curve too much in comparison to the data. Possible reasons for this are discussed later.

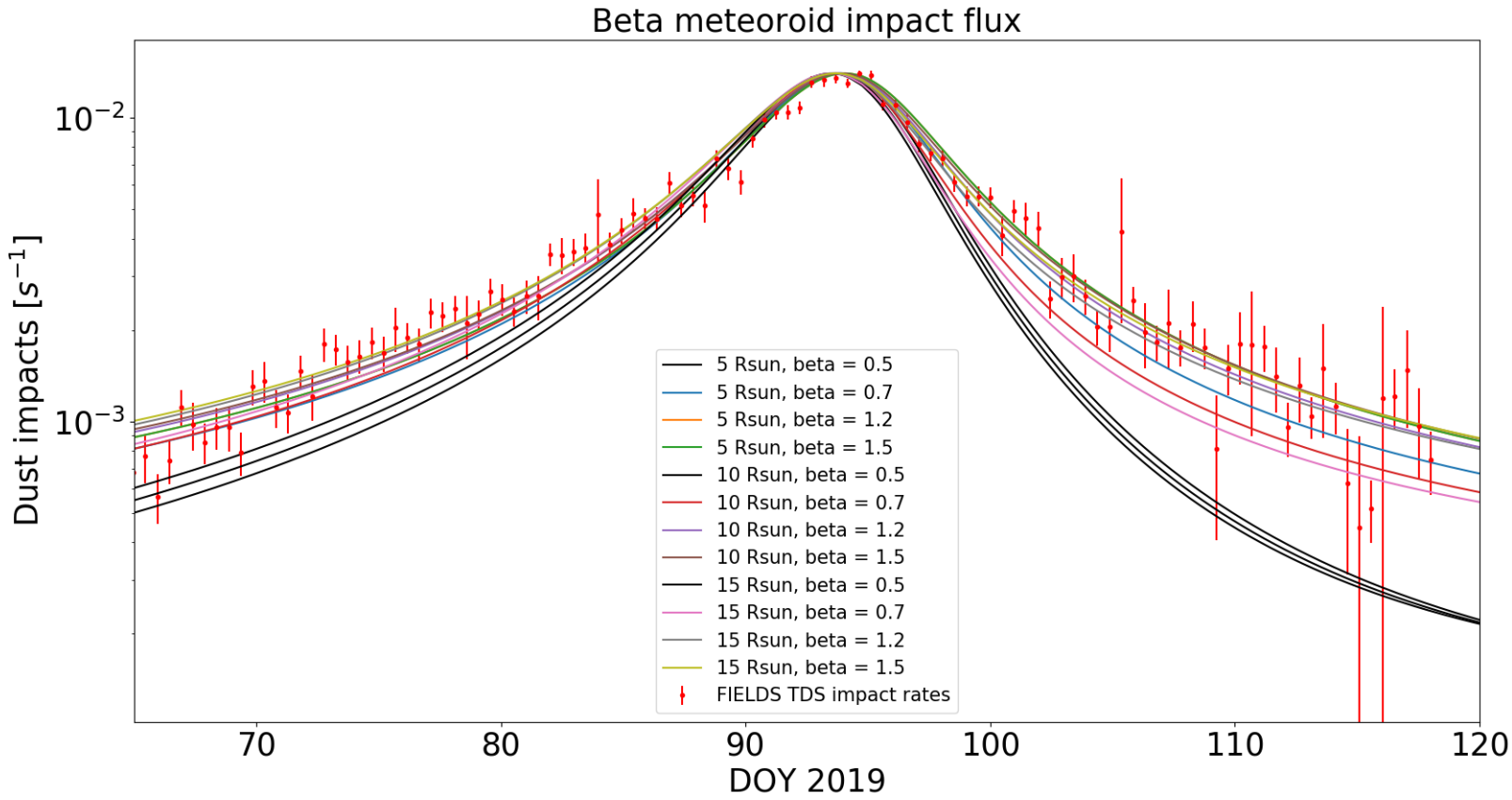

Figure 6.2: Calculated flux curves with PSP TDS impact rates for PSP's second orbit of the Sun. The flux curves are scaled to fit PSP TDS impact rates at perihelion. The red lines are the error bars of the impact rate measurements. The flux curves were calculated for radiation pressure to gravity ratios of 0.5, 0.7, 1.2 and 1.5, and production distances of 5, 10 and 15 R_{Sun}.

6.2.1 Best fit

To find the parameters that best describe the data, two different approaches to find a best fit were made. Firstly a non-linear least squares method was used to find a curve fit to the data, using the model (equation 5.1) of the dust flux that forms at a given distance from the Sun. Limits for the parameters were $\beta = [0.5, 2.0]$, $r_0 = [5, 20]$ R_{sun} and n_0 had no limit applied. The results show that the best parameters were $\beta = 1.98$, $r_0 = 12.22$ R_{Sun} and $n_0 = 0.45$ km^{-3} and it is shown in figure 6.3.

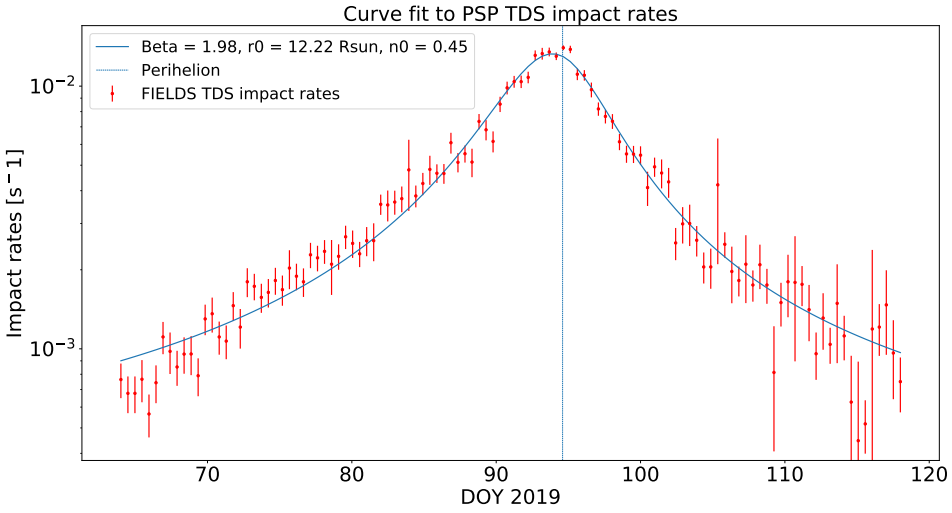

Figure 6.3: Curve fit to impact rates using a non-linear least squares method. Results for this model were $\beta = 1.98$, $r_0 = 12.22$ R_{sun} and $n_0 = 0.45$ km^{-3}.

Both the radiation pressure to gravity ratio and the production distance from the Sun of this fit are significantly higher than previous results. Szalay et al. (2020) used $r_0 = 5$ R_{sun} as the production distance for all their models, and explored radiation pressure to gravity ratio up to $\beta = 1.2$. The reason for the high radiation pressure to gravity ratio found here, could be that there are very small particles which are affected by electromagnetic forces which could slowly accelerate them radially outwards (Czechowski and Mann, 2010). This could lead to an observed particle with a higher radiation pressure to gravity ratio. Another point is that the assumed circular orbits of the parent objects might not be the most valid assumption to make. Most of the dust particles are produced from comets and asteroids in elliptical orbits (Mann et al., 2004). It is therefore reasonable to assume that dust particles in elliptical orbits are also a source of beta meteoroids. In this case, the production rates are high near perihelion of their orbit, where the dust density and collision rates are

the largest. The produced beta meteoroids would have a higher initial velocity than those produced from a circular orbiting parent object (Grün et al., 1985). This could lead to the model showing that higher radiation pressure to gravity ratios appears to fit better than what is really the case. Also, it is theoretically possible that dust particles with a volume fraction of above 14 % graphite have $\beta \geq 2$. Young cometary dust particles in the size range $10^{-14} - 10^{-13}$ g could also have a radiation pressure to gravity ratio of nearly 2 (Wilck and Mann, 1996). This could mean that meteoroids of a lower radiation pressure to gravity ratio than what is found by the best fit could give the same curve as the model predicts for such a high radiation pressure to gravity ratio.

Due to the difference in curvature between the inbound and outbound leg, a separate fit was made for each part. Figure 6.4 shows the same curve fitting procedure used on the inbound leg, and figure 6.5 shows the same on the outbound leg.

On the inbound leg it is again seen that the best fit to the data is a model with $\beta = 2$, $r_0 = 10.62\ R_{sun}$ and $n_0 = 0.41\ \text{km}^{-3}$. The model still curves more than the actual impact rates, suggesting that the reality differs from the model, given that tweaking the parameters won't give a better fit. On the outbound leg the model fits the data very good, given the parameters $\beta = 1.53$, $r_0 = 20\ R_{sun}$ and $n_0 = 0.81\ \text{km}^{-3}$. The radiation pressure to gravity ratio is only slightly higher than previous results, but the production radii r_0 is significantly higher. The quality of all fits can be found in figure 6.6 where the relative deviation from the data can be seen for every model. This is part of the model error analysis which is described in the next section.

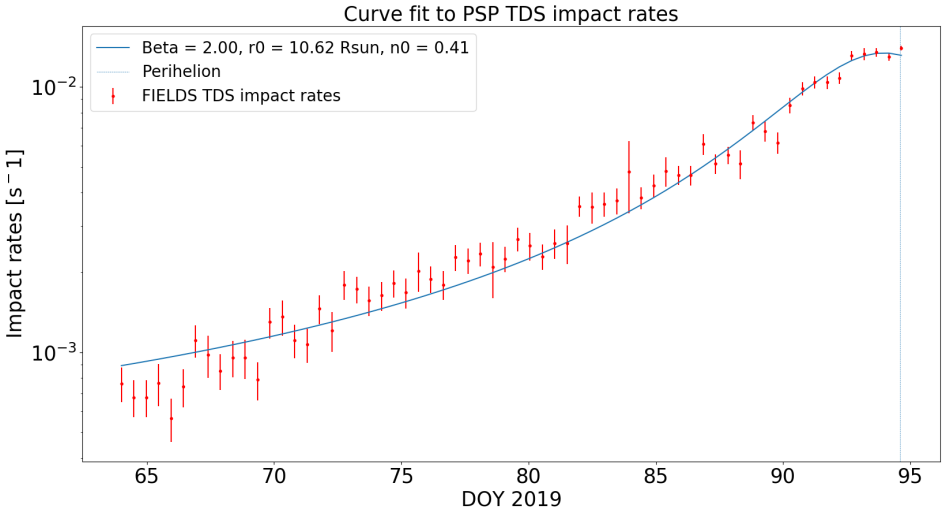

Figure 6.4: Best fit to the inbound leg of the orbit using a non-linear least squares method. Results for this fit were $\beta = 2.0$, $r_0 = 10.62\ R_{sun}$ and $n_0 = 0.41$ km^{-3}.

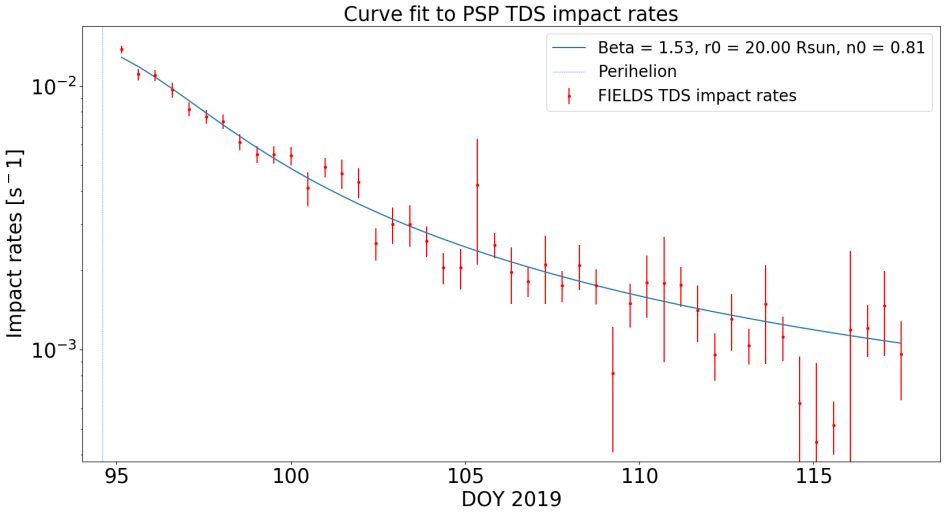

Figure 6.5: Best fit to the outbound leg of the orbit using a non-linear least squares method. Results for this fit were $\beta = 1.53$, $r_0 = 20\ R_{sun}$ and $n_0 = 0.81$ km^{-3}.

6.2.2 Model error analysis

Using a least squares method could over-emphasize detections which are far from the general trend of detections. Also the error measure does not take into account the error bars for each detection that are included in the data set. This means that the fit is much influenced by the outliers, which there are a few of on the outbound leg. Therefore, a second approach to finding a best fit was done, not using squares for the deviation from measurements, but rather the linear sum of deviates:

$$E = \frac{|m - d|}{m} \tag{6.1}$$

where E is the relative deviation between two points, m is the point determined from the calculated model and d is the point from FIELDS TDS impact rates. The deviation measure of each model was calculated as the average of E and n_0 was chosen from a range of values to be the one which gave the minimum deviation for each model. The range was 0.01 to 10 km^{-3}. In this way, all models considered were also scaled to fit the data. The results are shown in figure 6.6.

The relative deviation for a model with $\beta = 0.8$ and $r_0 = 5\ R_{sun}$ is $\simeq 16$ %, and for a model with $\beta = 2.0$ and $r_0 = 18\ R_{sun}$ it is $\simeq 14$ %. One can see that, given the uncertainties, little can be said for models of $\beta > 0.8$ as they all have a small relative deviation, and the differences between the models are insignificant. This could point to the fact that the impact rates measured by PSP do not agree with models assuming they only arise from one radiation pressure to gravity ratio and one production distance, because in reality they most probably arise from several different radiation pressure to gravity ratios and from a range of production distances from the Sun. What can be said is that beta meteoroids with $\beta < 0.6$ that are produced far away from the Sun do not agree with the observations.

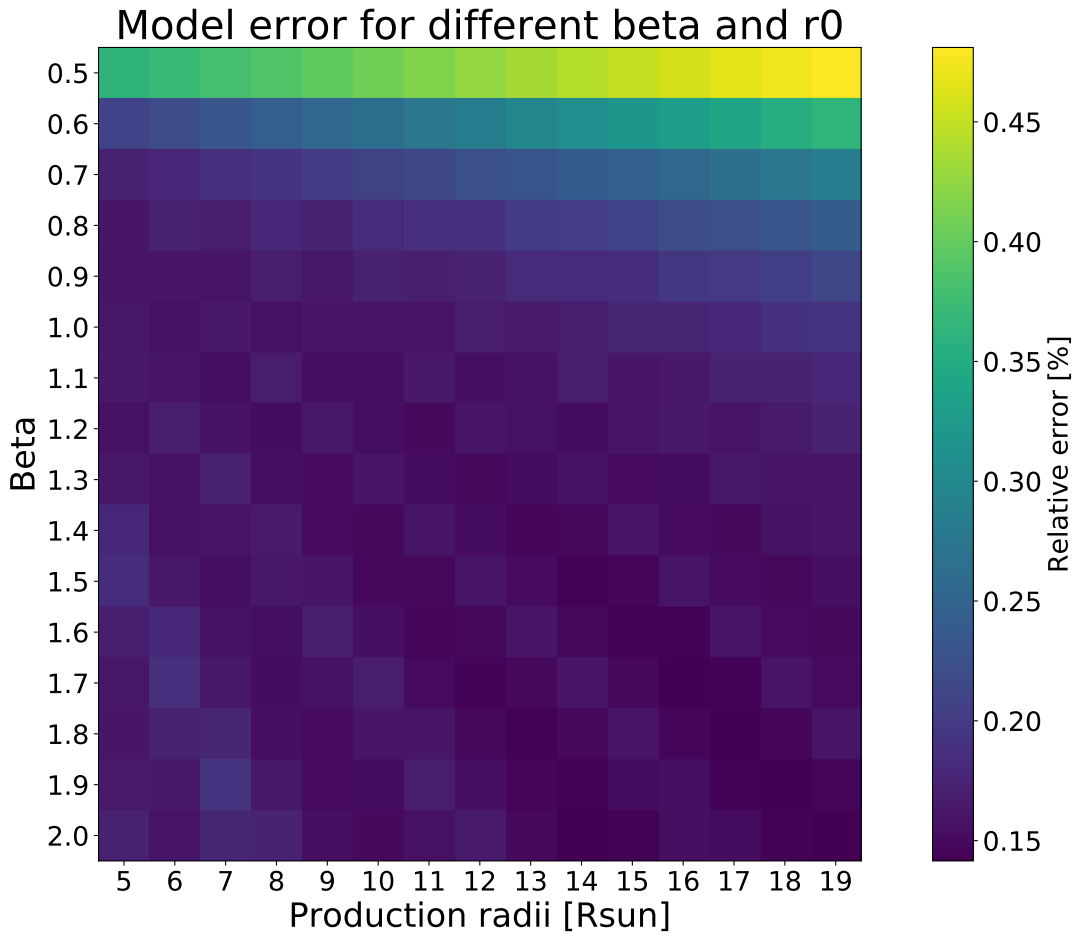

Figure 6.6: Calculated deviation (called "error" in figure) between different models and the FIELDS TDS data. Yellow and blue color corresponds to high and low deviation, respectively.

Figure 6.7 shows the radiation pressure to gravity ratio distribution over mass for young cometary dust particles that are highly absorbing and asteroidal dust particles that are less absorbing. The figure was adapted from Wilck and Mann (1996). The radiation pressure to gravity ratio values were calculated by the authors by simulating the light scattering and absorption properties of dust particles of different compositions over the solar spectrum. In addition to young cometary and asteroidal dust particles, the distribution was also calculated for old cometary and interstellar dust. The distributions for such particles is similar to the one for asteroidal dust particles. From the figure one can see that high beta occurs for a certain mass of particles. From this it is inferred that particles with a high radiation pressure to gravity ratio should be of a certain mass. Assuming most of the particles impacting PSP is young cometary dust, their mass range could be assumed to be from 10^{-16} to 10^{-12} g. Assuming a mass density of 2.5 g cm^{-3} and compact circular particles, the size range would be particles with radii of $\sim$ 0.02 µm to $\sim$ 0.5 µm. Thus particles within this size range can have a beta value of almost 2 if they are young cometary dust.

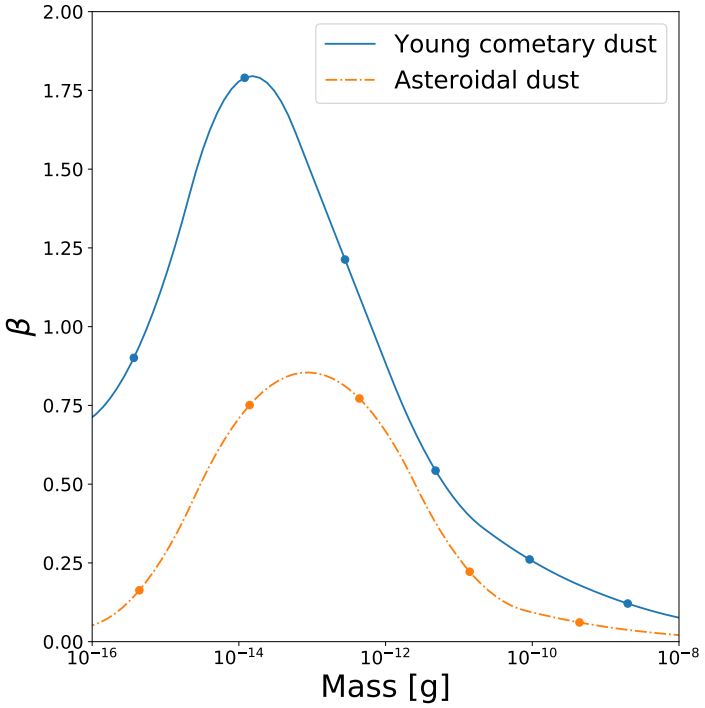

Figure 6.7: The radiation pressure to gravity ratio β as function of mass for young cometary dust and asteroidal dust particles. The figure is adapted from Wilck and Mann (1996) with the datapoints showing their calculated values and the lines are interpolated to guide the eye.

6.3 Dust impact signals

Unfortunately, only low resolution monopole data from PSP was available at this time. Nevertheless, an attempt was made to compare this data to the dust model describing the dust impact signal that was discussed in section 4.1.

Figure 6.8 shows three observations from the monopole data by PSP, assumed to be dust impacts, and a modeled dust impact pulse to fit to these observations. The two first dust impacts happened at 1st of November 2018 12:17 UTC within less than 5 seconds from one another, and the third on the 3rd of November 2018 12:17 UTC. PSP was for the first two at a heliocentric distance of $\sim$ 50 R_{Sun}, and $\sim$ 41 R_{Sun} for the last one.

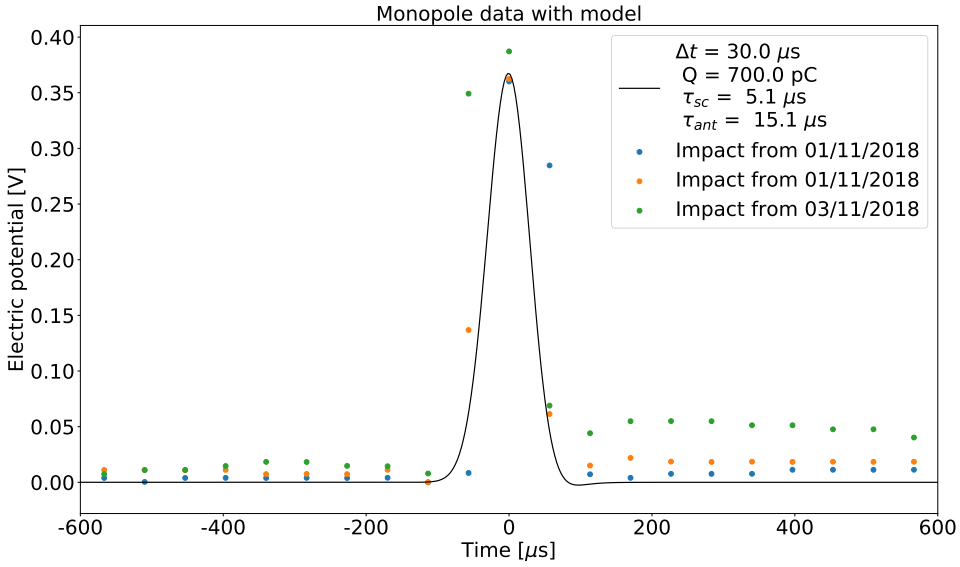

Figure 6.8: Three monopole signals observed from monopole PSP data, assumed to be dust impacts shown in blue, orange and green scatter plots. All signals are the potentials measured between antenna 1 (V1) and the spacecraft body. The black line shows a dust impact signal model with approximated parameters to fit the signals.

The observed signals have an amplitude of about 0.4 V. For the modeled dust impact, the charging timescale is assumed to be dependent upon the floating potential of the spacecraft, but is here chosen to fit the data at Δt = 30 µs which is a simplifying assumption. The relaxation time was calculated using solar wind parameters from 50 R_{sun} using equation 4.6, since two of the assumed dust impacts happened at $\sim$ 50 R_{sun} and the one from 03/11/2018 happened at

$\sim 41\ R_{sun}$. The result was $\tau_{sc} = 5.1$ µs. The relaxation time of the antenna was assumed to be slightly larger than the spacecraft, at $\tau_{sc} = 15.1$ µs. The charge production then determines the amplitude of the signal, and it is shown to fit well with a charge production of $Q \simeq 700$ pC. The model shows that for these parameters, there is almost no overshoot of the signal after the dust impact, which agrees with the data from the probe.

For a dust impact producing a charge of 700 pC it can be calculated what combination of radiation pressure to gravity ratios and production distances from the Sun a beta meteoroid needs to have to produce such a charge. This was calculated for radiation pressure to gravity ratios ranging from 0.5 to 2 and production distances from the Sun ranging from 5 to 20 R_{Sun}. The impact speed at 50 R_{Sun} was calculated for each beta meteoroid, and the mass was assumed to be on the order of 10^{-14} g. This assumption was made based on the variation of the radiation pressure to gravity ratio with mass from figure 6.7, and that high radiation pressure to gravity ratio dust fluxes fit the impact rates measured by PSP.

The result of the calculated charge production is shown in figure 6.9. The charge production was calculated from $Q = 0.7m^{1.02}v^{3.48}$ as discussed in section 4.2. The figure shows how the charge production, which influences the amplitude of the signal, varies with the distance where the particles are formed and with their radiation pressure to gravity ratio. The light blue/green diagonal area corresponds to a charge production of approximately $\sim$ 700 pC as is estimated from the antenna measurements. Particles with a too low radiation pressure to gravity ratio or that are produced too far out from the Sun have a low charge production when they impact the spacecraft (dark blue area). Similarly particles with a too high radiation pressure to gravity ratio that are produced close to the Sun will have a higher charge production when they impact the spacecraft (bright yellow area). It is seen that a beta meteoroid produced within 13 R_{Sun} which simultaneously has a radiation pressure to gravity ratio of more than 1 could have produced the signals.

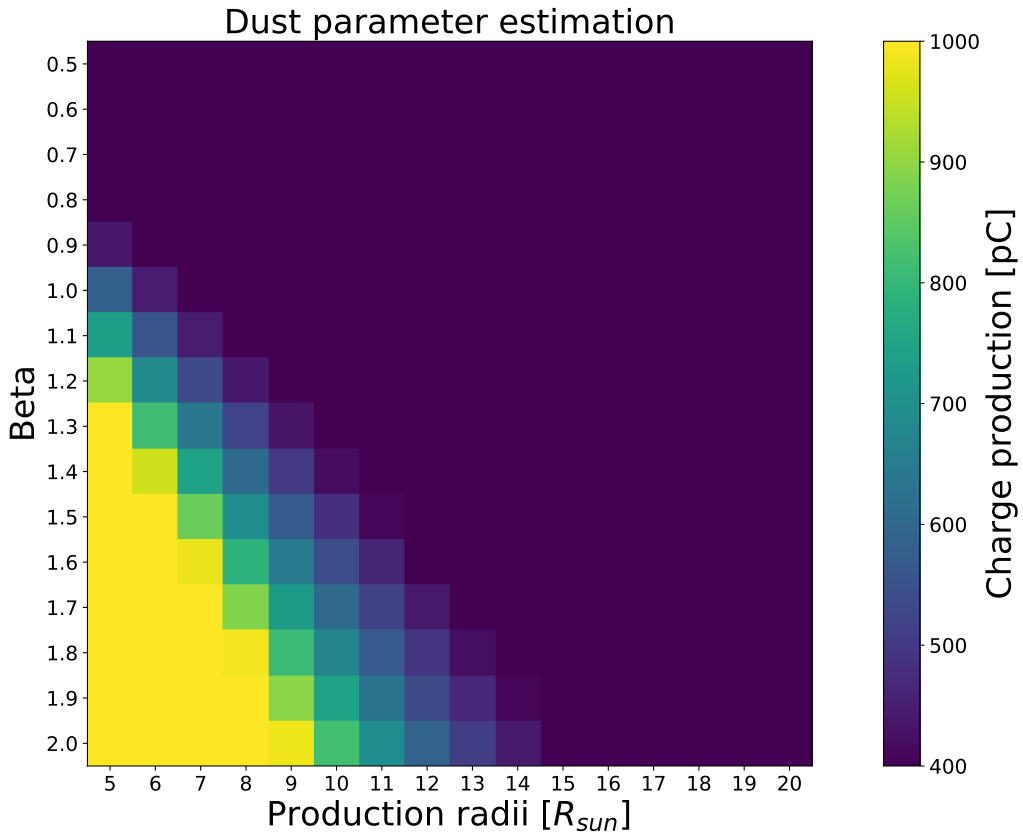

Figure 6.9: Calculated charge production for a range of radiation pressure to gravity ratios and production distances from the Sun. All dust particles were assumed to have a mass of 10^{-14} g.

7

Conclusion

For this master thesis the fluxes of beta meteoroids were calculated for different radiation pressure to gravity ratios and different production distances from the Sun. These calculations were compared to the observed impact rates by PSP. The result of the impact rates model agrees with previous studies (Szalay et al., 2020) that the impact rates recorded by PSP can be explained by beta meteoroids. The difference from previous studies is that both the radiation pressure to gravity ratio of the meteoroids and the production distance is shown to be greater. The analysis by Szalay et al. (2020) assumes radiation pressure to gravity ratios between 0.5 and 1.2. The radiation pressure to gravity ratios that were calculated for different dust properties by Wilck and Mann (1996) are 0.8 for most model assumptions i.e. asteroidal, old cometary and interstellar dust particles. The results from the flux and impact signal analysis points to beta meteoroids of higher radiation pressure to gravity ratios, which can be explained by young cometary dust. The curve fits point to a production distance outside of 10 R_{Sun}, and a radiation pressure to gravity ratio of above 1.5. For the entire section of the orbit a model with $\beta = 1.98$ and $r_0 = 12.22$ R_{Sun} is shown to be the best fit.

The model error analysis later shows that the curve fits do not separate themselves from other models as the clearly best fits. In fact the differences between models with $\beta > 0.7$ are so small that given the uncertainties they cannot be distinguished from each other. This points to the fact that most probably the impact rates measured by PSP consists of many different beta meteoroids with different radiation pressure to gravity ratios that are produced at different

distances from the Sun. The models with $\beta = 0.5$ do separate themselves from the other models as the worst fits to the data. The other models with a low radiation pressure to gravity ratio has to be produced close to the Sun in order to agree with the observations.

The conclusion is thus that the observed impact rates from PSP's second orbit is not well described by a single model calculated at a single production distance with one radiation pressure to gravity ratio. The observations could be more correctly estimated by a model which would take into account several beta meteoroids with different radiation pressure to gravity ratios and different production distances.

Three assumed dust impact signals were also considered and analyzed to estimate which dust particles could have made such signals. It was found that the signals could be produced by impacts of beta meteoroids which were produced within a distance of 13 R_{Sun} from the Sun and have a radiation pressure to gravity ratio of above 1. The radiation pressure to gravity ratio distribution with mass shows that the highest radiation pressure to gravity ratios occur for dust particles in the mass range $10^{-16} - 10^{-12}$ g. The impacts could be made by beta meteoroids in this mass range assumed to be young cometary dust, and an estimated signal of a beta meteoroid with $m = 10^{-14}$ g was shown to fit the signals. It was also shown that increasing the radiation pressure to gravity ratio must be met by an increase in production distance to agree with the approximated charge production for the dust impact signals measured by PSP. Similarly, a reduction in production distance must be met by a reduction in the radiation pressure to gravity ratio.

Further work should look into whether one could produce a model which takes into account different production rates for different distances and radiation pressure to gravity ratios. This might give a better approximation to the actual flux as it is, as shown, most probably from different beta meteoroids produced at different distances from the Sun. Once high resolution monopole data is released it could also be estimated what beta meteoroids are actually impacting PSP, in more detail. Once measurements made by PSP of the solar wind parameters are published, such as the electron density or the photelectron temperature, the charging timescale of the spacecraft Δt and the relaxation time τ could be estimated more accurately.

References

S. D. Bale, K. Goetz, P. R. Harvey, P. Turin, J. W. Bonnell, T. Dudok de Wit, R. E. Ergun, R. J. MacDowall, M. Pulupa, M. Andre, M. Bolton, J.-L. Bougeret, T. A. Bowen, D. Burgess, C. A. Cattell, B. D. G. Chandran, C. C. Chaston, C. H. K. Chen, M. K. Choi, J. E. Connerney, S. Cranmer, M. Diaz-Aguado, W. Donakowski, J. F. Drake, W. M. Farrell, P. Fergeau, J. Fermin, J. Fischer, N. Fox, D. Glaser, M. Goldstein, D. Gordon, E. Hanson, S. E. Harris, L. M. Hayes, J. J. Hinze, J. V. Hollweg, T. S. Horbury, R. A. Howard, V. Hoxie, G. Jannet, M. Karlsson, J. C. Kasper, P. J. Kellogg, M. Kien, J. A. Klimchuk, V. V. Krasnoselskikh, S. Krucker, J. J. Lynch, M. Maksimovic, D. M. Malaspina, S. Marker, P. Martin, J. Martinez-Oliveros, J. McCauley, D. J. McComas, T. McDonald, N. Meyer-Vernet, M. Moncuquet, S. J. Monson, F. S. Mozer, S. D. Murphy, J. Odom, R. Oliverson, J. Olson, E. N. Parker, D. Pankow, T. Phan, E. Quataert, T. Quinn, S. W. Ruplin, C. Salem, D. Seitz, D. A. Sheppard, A. Siy, K. Stevens, D. Summers, A. Szabo, M. Timofeeva, A. Vaivads, M. Velli, A. Yehle, D. Werthimer, and J. R. Wygant. The FIELDS Instrument Suite for Solar Probe Plus. *Space Science Reviews*, 204:49–82, 2016.

L. Calvinhac. Dust fluxes in the inner heliosphere. *Project Paper, Toulouse University*, 2019.

A. Czechowski and I. Mann. Formation and acceleration of nano dust in the inner heliosphere. *Astrophysical Journal*, 714(1):89, 2010.

H. Dietzel, G. Eichhorn, H. Fechtig, E. Grun, H. J.Hoffmann, and J. Kissel. The HEOS 2 and HELIOS micrometeoroid experiments. *Journal of Physics E: Scientific Instruments*, 6(3):209, 1973.

N. J. Fox, M. C. Velli, S. D. Bale, R. Decker, A. Driesman, R. A. Howard, J. C. Kasper, J. Kinnison, M. Kusterer, D. Lario, M. K. Lockwood, D. J. McComas, N. E. Raouafi, and A. Szabo. The Solar Probe Plus Mission: Humanity's First Visit to Our Star. *Space Science Reviews*, 204:7–48, 2016.

E. Grün, H.A. Zook, H. Fechtig, and R.H. Giese. Collisional balance of the meteoritic complex. *Icarus*, 62(2):244–272, may 1985.

E. Henriksen. Interplanetary dust flux near the Sun and estimates of dust fluxes onto the spacecraft Parker Solar Probe. *Project Paper, UiT*, 2019a.

E. Henriksen. The charge balance of spacecraft in the interplanetary medium and response to dust impacts. *Special Curriculum, UiT*, 2019b.

K. Issautier, N. Meyer-Vernet, M. Moncuquet, and S. Hoang. Solar wind radial and latitudinal structure: Electron density and core temperature from Ulysses thermal noise spectroscopy. *Journal of Geophysical Research: Space Physics*, 103(A2):1969–1979, 1998.

C. Leinert, M. Hanner, and E. Pitz. On the spatial distribution of interplanetary dust near 1 AU. *Astronomy and Astrophysics*, 63:183–187, 1978.

D. Malespina. Personal Communication. *PSP Dust Science Group Discussion*, 2020.

I. Mann, H. Kimura, D. A. Biesecker, B. T. Tsurutani, E. Grün, R. B. McKibben, J. Liou, R. M. MacQueen, T. Mukai, M. Guhathakurta, and P. Lamy. Dust Near The Sun. *Space Science Reviews*, 110(3/4):269–305, 2004.

I. Mann, L. Nouzák, J. Vaverka, T. Antonsen, Å. Fredriksen, K. Issautier, D. Malaspina, N. Meyer-Vernet, J. Pavlů, Z. Sternovsky, J. Stude, S. Ye, and A. Zaslavsky. Dust observations with antenna measurements and its prospects for observations with Parker Solar Probe and Solar Orbiter. *Annales Geophysicae Discussions*, pages 1–39, jul 2019.

N. McBride and J. A.M. McDonnell. Meteoroid impacts on spacecraft: Sporadics, streams, and the 1999 Leonids. *Planetary and Space Science*, 47(8-9):1005–1013, 1999.

D. J. McComas, M. Velli, W. S. Lewis, L. W. Acton, M. Balat-Pichelin, V. Bothmer, R. B. Dirling, W. C. Feldman, G. Gloeckler, S. R. Habbal, D. M. Hassler, I. Mann, W. H. Matthaeus, R. L. McNutt, R. A. Mewaldt, N. Murphy, L. Ofman, E. C. Sittler, C. W. Smith, and T. H. Zurbuchen. Understanding coronal heating and solar wind acceleration: Case for in situ near-Sun measurements. *Reviews of Geophysics*, 45(1), mar 2007.

N. Meyer-Vernet. Detecting dust with electric sensors in planetary rings, comets and interplanetary space. *Spacecraft Charging Technology*, 746:635, 2001.

N. Meyer-Vernet. *Basics of the Solar Wind*. Cambridge University Press, 2007.

NASA. Parker Solar Probe, 2019. URL `http://parkersolarprobe.jhuapl.edu/`.

Last accessed on 29/06/2019.

J. R. Szalay, P. Pokorný, S. D. Bale, E. R. Christian, K. Goetz, K. Goodrich, M. E. Hill, M. Kuchner, R. Larsen, D. Malaspina, D. J. McComas, D. Mitchell, B. Page, and N. Schwadron. The Near-Sun Dust Environment: Initial Observations from Parker Solar Probe. *The Astrophysical Journal Supplement Series*, 246 (2):27, 2020.

J. Vaverka, A. Pellinen-Wannberg, J. Kero, I. Mann, A. De Spiegeleer, M. Hamrin, C. Norberg, and T. Pitkanen. Potential of earth orbiting spacecraft influenced by meteoroid hypervelocity impacts. *IEEE Transactions on Plasma Science*, 45(8):2048–2055, 2017.

E. C. Whipple. Potentials of surfaces in space. *Reports on Progress in Physics*, 44(11):1197, 1981.

M. Wilck and I. Mann. Radiation pressure forces on "typical" interplanetary dust grains. *Planetary and Space Science*, 44(5):493–499, 1996.

M. C. Wyatt. *Dynamics of Small Bodies in Planetary Systems*, volume 758 of *Lecture Notes in Physics*. Springer Berlin Heidelberg, Berlin, Heidelberg, 2009.

A. Zaslavsky. Floating potential perturbations due to micrometeoroid impacts: Theory and application to S/WAVES data. *Journal of Geophysical Research: Space Physics*, 120(2):855–867, 2015.

H. A. Zook and O. E. Berg. A source for hyperbolic cosmic dust particles. *Planetary and Space Science*, 23(1):183–203, jan 1975.

A

Appendix

A.1 Abstracts of previous work

A.1.1 Project paper (Henriksen, 2019a)

The main dust production, distribution and destruction effects in the inner heliosphere are presented. Further, the Parker Solar Probe's methods for detecting dust particles with the FIELDS instrument, and beta meteoroids, are discussed. A program to calculate dust trajectories is used to estimate impact speeds onto Parker Solar Probe. To calculate the dust trajectories it was assumed that the particles were produced by colissional fragmentation and with a parent object on a circular orbit in the ecliptic. The production is assumed to be evenly distributed around the Sun. Hyperbolic orbits are calculated for dust fragments produced at 5, 10 and 15 solar radii and their relative impact speeds are calculated for the first perihelion pass of Parker Solar Probe in the Heliocentric Earth Ecliptic coordinate system. It is shown that particles produced at 5 solar radii will have significantly higher impact speed than those produced at 10 or 15 solar radii. [...]

A.1.2 Special curriculum (Henriksen, 2019b)

The goal of this work is to understand how dust impacts can be detected using antenna measurements onboard the Parker Solar Probe (PSP) spacecraft. The spacecraft is electrically charged and after a dust impact its potential

changes for a short time, which can be noticed in radio wave measurements with antennas. To describe the signal generated by a dust impact, a model is used that Zaslavsky et. al (2015) developed to describe measurements of the STEREO spacecraft near 1 AU. The time scales for the spacecraft to reach the floating potential again determine the signal shape and these timescales depend on the parameters of the ambient solar wind. The spacecraft floating potential and the charging currents are described for PSP. The dust impact signals are estimated for different solar wind conditions, charge productions, and dust particle sizes. The model is used to predict how signals that PSP might produce during its first perihelion pass of the Sun will look like. It is found that for an unbiased measurement, particles with a mass of less than 4×10^{-12} grams will produce signals that can be hard to detect. Particles smaller by one order of magnitude will produce signals that are also weaker by one order of magnitude. These estimates are made assuming an average impact speed of the dust particles of $v(r) = v_0 \left(\frac{r}{r_0}\right)^{-\frac{1}{2}}$ where v_0 is the average impact speed at 1 AU and r_0 is 1 AU. [...]

A.2 Code

All code included in this section was written by the author in Python and is included for transparency, and in case it could be helpful to the reader.

A.2.1 Functions

The code in this section consists of functions used to calculate different parameters used in the analysis. The functions for calculating i.e. the impact speed from equation 5.9 and the impact rates from equation 5.1 are included. The code includes brief descriptions of the function itself and a description of the parameters required to do the calculation in the docstring of the function.

```
# FUNCTIONS
import numpy as np

def beta_speed(beta,r0,distance):
  """
  Calculate speed of beta meteoroid on hyperbolic orbit with
                                  beta > 0.5

  Input:
    beta - beta value
    r0 - production radii
    distance - distance vector for which to calculate speed
```

```
  Output:
    v - total speed
    vr - radial speed
    vphi - azimuthal speed

  """

  mu = 1.38e20 # Gravitational parameter
  vr = np.sqrt(2*mu*((beta-0.5)/r0 + (1-beta)/distance - r0/(2*
                                    distance**2)))
  vphi = np.sqrt(mu*r0)/distance
  v = np.sqrt(vr**2 + vphi**2)

  return v, vr, vphi



def impactspeed(beta,distance,r,perp_speed):
  """
  Calculate impact speed for PSP and hyperbolic dust particles

  Input:
  beta : dust particle beta value
  distance: heliocentric distance to PSP [m]
  r: beta meteoroids production distance in [R_sun]
  perp_speed : PSP speed perpendicular to ecliptic

  Output:
  v_imp [km/s]
  """


  Rsun = 6.957e8 # [m] Sun radii: 700 000 km
  AU = 149597870700 # [m] Astronomical unit ~ 150 million km
  mu = 1.327e20 # GM = gravitational constant times mass of the
                                     Sun
  r0 = r*Rsun # Send value into function instead of defining
                                    within function

  # PSP orbital elements
  a = 0.5520*AU
  e = 0.6994

  # If distance is a vector and not just a number
  if isinstance(distance,np.ndarray):
    # Index of perihelion
    ind = int(np.argwhere(distance==np.min(distance)))

    # Different distance vectors for inbound/outbound
    r_inbound = distance[0:ind]
    r_outbound = distance[ind-1:-1]

    # Radial impact speed for inbound/outbound
    v_r_inbound = np.sqrt(2*mu*((beta-0.5)/r0+(1-beta)/
```

```
                                r_inbound-r0/(2*r_inbound**2)))
                                 + np.sqrt((mu*(2/r_inbound-1/a
                                -(a*(1-e**2))/r_inbound**2)))
    v_r_outbound = np.sqrt(2*mu*((beta-0.5)/r0+(1-beta)/
                                r_outbound-r0/(2*r_outbound**2)
                                )) - np.sqrt((mu*(2/r_outbound-
                                1/a-(a*(1-e**2))/r_outbound**2)
                                ))


    # Put inbound and outbound radial velocity vectors together
                                 into 1 vector
    v_r = np.concatenate((v_r_inbound,v_r_outbound))

    # If distance is only one number
  else:
    v_r = np.sqrt(2*mu*((beta-0.5)/r0+(1-beta)/distance-r0/(2*
                                distance**2))) + np.sqrt((mu*(2
                                /distance-1/a-(a*(1-e**2))/
                                distance**2)))

  # Angular impact speed
  v_phi = np.abs(np.sqrt(mu)/distance *(np.sqrt(r0)-np.sqrt(a*(
                                1-e**2))))


  v_imp = np.sqrt(v_r**2 + v_phi**2 + perp_speed**2)

  return v_imp/1e3


def impactrates(n0,distance,impactspeed):

  """
  Calculate dust impact rate onto PSP during orbit 2

  Input:
  n0: dust density value at 1 AU [km^-3]
  distance: PSP heliocentric distance vector [m]
  impactspeed: Hyperbolic dust impact speeds along orbit [km/s]


  Output: Flux impact rates [s^-1]
  """


  AU = 149597870700 # [m] Astronomical unit ~ 150 million km

  density = n0/1e9 # Convert to [m^-3]
  v = impactspeed*1e3 # Convert to [m/s]

  n = density/(distance/AU)**(2)

  # Assuming all dust particles hit the heat shield:
```

```
  A = np.pi*(1.15/1)**2 # m^2

  # Calculate flux impact rate:
  R = n*v*A

  return R



def signalestimate(delta_t, Q, tau_sc, tau_ant):

  """
  Estimates the potential perturbation of a dust impact given
                                the parameters:

  C_sc: Spacecraft capacitance [F]
  C_ant: Antenna capacitance [F]
  delta_t: Charging time of dust impact
  Q: Total charge collected
  tau_sc: Spacecraft relaxation time
  tau_ant: Antenna relaxation time

  Outputs:

    t - Time vector [s]
    dphi - Potential perturbation [V]

  """

  C_sc = 200e-12
  C_ant = 60e-12

  t = np.linspace(-1.36e-3,1.36e-3,1000)    # change this to
                                same timescale as signal data
                                with equal #samples

  # Proportion of charging happening at the antenna
  proportion_ant = 0.05

  ### Discrete convolution, summation variable m
  m = np.linspace(0,0.01,len(t))
  dm = m[5]-m[4]              # Sampling rate (5 and 4 are
                                arbitrary values)
  expfunc_sc = np.exp(-m/tau_sc)
  expfunc_ant = np.exp(-m/tau_ant)

    # Allocate variables
  dphi_sc = np.zeros(len(t))
  dphi_ant = np.zeros(len(t))
  I = np.zeros((len(t),len(m)))

  # Perform convolution, I is current I_dust
  for i in range(len(t)):
```

```
    I[i,:] = ((-Q)/(np.sqrt(2*np.pi)*delta_t))*np.exp((-(t[i]-m
                                )**2)/(2*delta_t**2))
    dphi_sc[i] = (1-proportion_ant)/C_sc * np.sum(expfunc_sc *
                                I[i,:])
    dphi_ant[i] = proportion_ant/C_ant * np.sum(expfunc_ant * I
                                [i,:])

# Multiply by sampling rate to scale values correctly
dphi_sc = dphi_sc * dm
dphi_ant = dphi_ant * dm
dphi = dphi_ant-dphi_sc

# Return time vector and signal
return t,dphi
```

A.2.2 Scripts

The following script is used to produce the results given in the model error analysis, figure 6.6. The script uses functions given above to load PSP position data, load PSP TDS data, calculate impact speeds and impact rates for all beta and production distances, and then calculate the relative deviation of the models to the PSP TDS data. The results are saved in numpy (Python library) files containing the deviations for all production distances for each radiation pressure to gravity ratio.

```
import numpy as np
import functions # file containing all my functions
import multiprocessing as mp

# Load PSP orbit coordinates ASCII file
Coordinates2D,Coordinates3D = functions.PSPdata_load('
                                PSP_Orbit2_HEE_from04march-
                                80days.txt')

# Make distance vector from PSP 3D orbit data
distance = np.sqrt(Coordinates3D[:,0]**2 + Coordinates3D[:,1]**
                                2 + Coordinates3D[:,2]**2)

# DOY vector
DOY_2 = np.linspace(63,143,len(distance))

# Calculate PSP speed perpendicular to ecliptic plane
v = np.zeros(Coordinates3D.shape[0])
v_perp = np.zeros(Coordinates3D.shape[0])
for i in range(Coordinates3D.shape[0]-1):
    v[i] = (Coordinates3D[i+1,2] - Coordinates3D[i,2])/60 #
                                    Each sample is spaced by 60
                                     seconds
    v_perp[i] = np.sqrt(v[i]**2)

# Import PSP TDS data
rates, DOY, error = functions.TDS_load()

n0 = np.arange(1e-2,10,0.01)     # Define n0 value range:
beta = np.arange(0.5,2.1,0.1)    # Beta values
r0 = np.arange(5,20,1)           # Production distance [Rsun]
AU = 149597870700                # Astronomical unit [m] ~ 150
                                 million km

# Use multiprocessing to make program run faster
cores = mp.cpu_count()
pool = mp.Pool(cores)

# Produce fluxes for all beta, r0, n0
model = [] # list to be filled with model data
for betaval in beta:
    results = {} # dictionary
```

```
    for radii in r0:
        results['r0_%d' % radii] = [] # lists inside dictionary
        speed = functions.impactspeed(betaval,distance,radii,
                                      v_perp)

        # Calculate model without density:
        model_nodens = functions.impactrates_nodensity(distance
                                      ,speed)
        for density in n0:
            # Scale impact rate model by density, then
                                          calculate error
            density = density/1e9 # Convert to [m^-3]
            n = density/(distance/AU)**2
            model = model_nodens*n # Scale with density
            avgerr = pool.starmap(functions.error, [(np.array(
                                          model).flatten(),
                                          DOY_2,rates,DOY)])
            results['r0_%d' % radii].append(avgerr)

    np.save('/results/results_beta_%s' % betaval, results) #
                                    Save results
    results = None # Reset variable
```

The following script uses functions to calculate and plot speed profiles of beta meteoroids shown in figure 3.2. It also calculates and plots the charge production estimation shown in figure 6.9. Lastly it interpolates given values from Wilck and Mann (1996) to produce the radiation pressure to gravity ratio over mass distribution shown in figure 6.7.

```
import numpy as np
import functions
import matplotlib.pyplot as plt

'''
Calculates and plots speedprofiles for beta meteoroids.
Calculates and plots estimated charge production for selected
                                impact signals from PSP.
Interpolates radiation pressure to gravity ratio values from
                                Wilck & Mann (1996) and
                                produces
figure for young cometary dust and asteroidal dust.

'''


#### Calculate and plot beta meteoroid speed profiles

AU = 149597870700 # [m] Astronomical unit ~ 150 million km
Rsun = 6.957e8 # [m] Sun radii: 700 000 km

distance = np.linspace(0.01,1,10000)*AU
```

```
beta = [0.5,1.0,1.5]
r0 = [10]
colors = ['red','green','blue','black']
style =  [':','-','-.']
k = 0
fig, axs = plt.subplots()
for i,bet in enumerate(beta):
  for j,r in enumerate(r0):
    col = colors[k]
    v,vr,vphi = functions.beta_speed(bet,r*Rsun,distance)
    axs.plot(distance/AU,v/1e3, linestyle = style[1], color =
                                col, label='total speed, $\\
                                beta$ = %.1f, $r_0$ = %d $R_{
                                sun}$' % (bet,r))
    k = k+1


axs.set_title('Beta meteoroid speed profile', fontsize=25)
axs.legend(loc='right', fontsize=19)
plt.xlabel('Distance [AU]',fontsize=25)
plt.ylabel('Speed [km/s]', fontsize=25)
plt.yscale('log')
plt.xticks(fontsize=25)
plt.yticks(fontsize=25)
axs.tick_params(axis= 'y', which='minor', labelsize=25)
plt.show()



####### Calculate impact speed of PSP to beta meteoroid signals
                                and estimate charge production

distance = 50*Rsun # Heliocentric distance of impact
betas = np.arange(0.5,2.1,0.1).round(1) # Beta value
r0s = np.arange(5,21,1) # Beta meteoroid production distance [
                                Rsun]
perp_speed = 0

m = 1e-17 #[kg]
print(len(betas),len(r0s))
Q = np.zeros((len(betas),len(r0s)))

for i,beta in enumerate(betas):
  for j,r0 in enumerate(r0s):
    impspd = functions.impactspeed(beta,distance,r0,perp_speed)
    Q[i,j] = (0.7*m**1.02*impspd**3.48)*1e12 # [pC]


fig2, ax2 = plt.subplots()
im = ax2.imshow(Q)
im.set_clim(400,1000)
plt.xticks(np.arange(0, 16, step=1),r0s)
plt.yticks(np.arange(0, 16, step=1),betas)
cbar = fig2.colorbar(im)
```

```
cbar.set_label('Charge production [pC]', fontsize=25)
plt.title('Dust parameter estimation',fontsize=25)
plt.xlabel('Production radii [$R_{sun}$]', fontsize=25)
plt.ylabel('Beta', fontsize=25)
ax2.tick_params(axis='both', which='major', labelsize=15)
ax2.tick_params(axis='both', which='minor', labelsize=15)
cbar.ax.tick_params(labelsize=15)
plt.show()


# Reproduce Wilck beta mass figure
from scipy.interpolate import interp1d

# Values for young cometary dust from Wilck & Mann (1996)
beta_youngcomet = np.array([0.768, 0.901, 1.790, 1.213, 0.543,
                            0.261, 0.121, 0.049])
mass_youngcomet = np.array([1.2e-17, 3.7e-16, 1.2e-14, 2.8e-13,
                             4.8e-12, 9.2e-11, 2.0e-9, 5.0e
                            -8])

# Values for asteroidal dust from Wilck & Mann (1996)
beta_asteroid = np.array([0.106, 0.163, 0.751, 0.772, 0.222, 0.
                            061, 0.018, 0.005])
mass_asteroid = np.array([1.4e-17, 4.4e-16, 1.4e-14, 4.4e-13, 1
                            .4e-11, 4.4e-10, 1.4e-8, 4.4e-7
                            ])

x = np.log(mass_youngcomet)
y = beta_youngcomet

# Interpolate
xnew = np.linspace(np.min(x),np.max(x),100)
f = interp1d(x, y, kind='quadratic')
y_smooth=f(xnew)

fig, ax = plt.subplots()
plt.scatter(np.exp(x), y)
plt.plot(np.exp(xnew), y_smooth, label='Young cometary dust')
plt.ylim(0,2)
plt.xlim(1e-16, 1e-8)
plt.xscale('log')
plt.xlabel('Mass [g]', fontsize=25)
plt.ylabel('$\\beta$', fontsize= 25)
ax.tick_params(axis='both', which='major', labelsize=15)
ax.tick_params(axis='both', which='minor', labelsize=15)


# FOR ASTEROIDAL DUST
x = np.log(mass_asteroid)
y = beta_asteroid

# Interpolate
xnew = np.linspace(np.min(x),np.max(x),100)
f = interp1d(x, y, kind='quadratic')
```

```
y_smooth=f(xnew)

plt.scatter(np.exp(x), y)
plt.plot(np.exp(xnew), y_smooth, '-.', label='Asteroidal dust')
plt.legend(fontsize=20)
plt.show()
```